PB85-237857

Surrogate Experimental Models for Studying Particle Deposition in the Human Respiratory Tract

(U.S.) Health Effects Research Lab.
Research Triangle Park, NC

Aug 85

U.S. Department of Commerce
National Technical Information Service
NTIS

PB85-237857

EPA/600/D-85/158
August 1985

Surrogate Experimental Models for Studying Particle Deposition in the Human Respiratory Tract

by

T. Blayne Martonen
Toxicology Branch
Health Effects Research Laboratory
Research Triangle Park, NC 27711

Health Effects Research Laboratory
Office of Research and Development
U.S. Environmental Protection Agency
Research Triangle Park, NC 27711

REPRODUCED BY
NATIONAL TECHNICAL
INFORMATION SERVICE
U.S. DEPARTMENT OF COMMERCE
SPRINGFIELD, VA. 22161

TECHNICAL REPORT DATA *(Please read Instructions on the reverse before completing)*		
1. REPORT NO. EPA/600/D-85/158	2.	3. RECIPIENT'S ACCESSION NO. PB85 237857/AS
4. TITLE AND SUBTITLE SURROGATE EXPERIMENTAL MODELS FOR STUDYING PARTICLE DEPOSITION IN THE HUMAN RESPIRATORY TRACT		5. REPORT DATE August 1985 6. PERFORMING ORGANIZATION CODE
7. AUTHOR(S) T. BLAYNE MARTONEN		8. PERFORMING ORGANIZATION REPORT NO.
9. PERFORMING ORGANIZATION NAME AND ADDRESS EPA,HERL,ITD,TB RTP, NC 27711		10. PROGRAM ELEMENT NO. AAGA1D 11. CONTRACT/GRANT NO.
12. SPONSORING AGENCY NAME AND ADDRESS Office of Research & Development Health Effects Research Laboratory USEPA Research Triangle Park, NC 27711		13. TYPE OF REPORT AND PERIOD COVERED 14. SPONSORING AGENCY CODE EPA-600/11
15. SUPPLEMENTARY NOTES		

16. ABSTRACT

Hazard assessment following challenge by ambient aerosols requires accurate estimation of exposure, that is, determination of the total mass of particulate matter deposited within the respiratoray tract, and its intercompartmental distribution. Aerosol deposition studies utilizing human test subjects yield valuable information on the deposition of inhaled particles in man, but experimental regimens lack the resolution to quantitate "hot spots" within the lung. Aerosol deposition experiments with respiratory tract surrogates, or models, can be designed to be complimentary to human studies. We have put experimental modelling efforts into perspective per their applicability for the risk assessment of inhaled ambient aerosols. Heterogeneity of deposition has been detected in in vitro experiments over a wide range of particulate sizes and flow rate magnitudes--in a variety of surrogate larynx-TB models, for both constant and time-dependent flow patterns, and for both phases (inspiration and expiration) of a breathing cycle. Hence, it is suggested that aerosol maldistribution in the human respiratory tract is an important element to be incorporated into future hazard assessment analyses of pollutant aerosols in the ambient and occupational environments.

17. KEY WORDS AND DOCUMENT ANALYSIS		
a. DESCRIPTORS	b. IDENTIFIERS/OPEN ENDED TERMS	c. COSATI Field/Group
18. DISTRIBUTION STATEMENT Unclassified	19. SECURITY CLASS *(This Report)* Release to Public 20. SECURITY CLASS *(This page)* Release to Public	21. NO. OF PAGES 59 22. PRICE

EPA Form 2220-1 (Rev. 4-77) PREVIOUS EDITION IS OBSOLETE

NOTICE

This document has been reviewed in accordance with U.S. Environmental Protection Agency policy and approved for publication. Mention of trade names or commercial products does not constitute endorsement or recommendation for use.

INTRODUCTION

The presence of irritant and toxic contaminants in the atmosphere poses potential hazards to the health and well being of the general population. Workers may receive additional exposures to materials of health effects concern upon the inhalation of ambient particles produced in mining and industrial processes. Airborne pollutants present not only a threat to the respiratory tract per se, but to other organs since the lung serves as the channel by which toxic materials are dispersed throughout the body via the lymphatic and circulatory systems or through mucociliary clearance and then swallowing.

In 1964 [1], the International Radiological Protection Commission established the Task Group on Lung Dynamics (TGLD) whose charter was to provide a sound scientific basis for a lung dosimetry model concomitant with the setting of inhalation exposure limits. The TGLD recommended that the human respiratory tract be visualized as consisting of three components. (i) Nasopharynx (NP)--defined as beginning at the anterior nares and extending through both the anterior and posterior pharynx to the epiglottis and larynx. In current parlance this compartment is commonly termed "extrathoracic", and distinctions are made between nasopharyngeal and oropharyngeal regions when considering breathing via the nose and mouth, respectively. (ii) Tracheobronchial (TB)--defined as the nonalveolated bronchial airways inclusive of, and between, the trachea and terminal bronchioles. These conducting airways are lined with a ciliated epithelium that is covered with mucus. (iii) Pulmonary (P)--defined as the functional, i.e., gas-exchange, region of the lung consisting of respiratory bronchioles, alveolar ducts and alveolar sacs. This compartment is lined with a non-ciliated epithelium that is covered

with surfactant. Particles deposited on surfaces within the NP and TB compartments are cleared, or removed, by the mucociliary system. In the P compartment, clearance occurs by macrophage action.

Hazard assessment following challenge by ambient aerosols requires accurate estimation of exposure, that is, determination of the total mass of particulate matter deposited within the respiratory tract. Since the various compartments have clearance mechanisms that differ in effectiveness and rate of action, it is important that the intercompartmental distribution of total respiratory tract burden be known as well. Indeed, as documented in following text, the most relevant factor to be considered in hazard evaluation may be the intracompartmental distribution of deposited aerosol mass since the occurrence of sites of enhanced particulate accumulation within airways, due to preferential deposition at selected locations and/or impaired clearance, will lead to increased exposure of nearby cells.

Aerosol deposition studies utilizing human test subjects yield valuable information on the disposition of inhaled particles in man. Systematic studies quantitating the effects of different factors on particle deposition, however, have been limited to a few institutions because of the complexity of the experimental work, the necessity of custom scientific instrumentation, the time consuming and financial requirements of the work, etc. Perhaps the most significant limitations of the human subject experiments are that current equipment used to measure radiolabelled-particle deposition lack the resolution to quantitate "hot spots" within the lung and that working with human subjects precludes extensive testing to delineate the behavior of inhaled aerosols.

Attempts to simulate in vivo aerosol deposition in man may be broadly divided into either predictive or experimental modelling efforts. These categories, however, are not mutually exclusive. For example, two distinct kinds of predictive models describe particle deposition with either laboratory-data-based empirical equations, or theoretically-based mathematical formulae and computer codes. Experimental, or laboratory, models may also be subdivided into two types: those in which attempts are made to maintain faithful simulations of morphology and those whose intent is to reproduce only particle deposition-efficiency characteristics. Each type of model has advantages and limitations; at present there is no "ultimate" model. Therefore, predictive and experimental modelling efforts should interface so as to more accurately simulate inhaled aerosol deposition.

In the balance of this text, we will attempt to put experimental modelling efforts into perspective per their applicability for the risk assessment of inhaled ambient aerosols. Aerosol deposition experiments with respiratory tract surrogates, or models, can be designed to be complimentary to human studies. Once validated by comparison to available data from in vivo tests, the surrogates can be used to supplement data describing aerosol deposition, for example, to measure "hot spot" intensities within branching airway models. This work is not presented as a definitive review of the subject matter. Rather, its purpose is to illustrate the wide variety of experimental models conceived by various authors in attempts to describe the fate of inhaled aerosols in man.

ARCHETYPE LUNGS

The geometry of the human respiratory system is quite complex (Figure 1). Here, it will be worthwhile to briefly highlight the chronological development of attempts to analytically describe TB morphology. First, it will be necessary to define applicable terminology. The lung is a serially branching network from the trachea to the alveolar sacs. The network per se is usually conceived as a successive array of tubes (rigid, right circular cylinders). Each array is considered as a "region" (Findeisen [4]) or "generation" (Weibel [5]) of the network. An airway at any given location within the network is a "parent" that branches, or divides, into downstream "daughter" airways which are termed "sisters". The most distinctive differences between the morphologies proposed by various authors are in: (i) numerical mode of division, i.e., dichotomous, etc., and (ii) compositional mode of division, i.e., symmetric (identical daughters), or asymmetric. Within an array, orientations of the tubes are defined in a relative sense (describing the change in airflow direction between successive parent and daughter tubes)--termed the branching angle, and in an absolute sense (describing a tube's angle with respect to the horizontal)--termed the gravity angle.

Perhaps the earliest lung geometry proposed for modelling purposes was that of Findeisen [4]. The lung was conceived as consisting of nine different regions. Within a region the tubes were identical and characterized by a specific diameter and length, which varied from region to region as did the number of tubes. The idealized branching scheme is given in Table I. The regions are connected in series following an abstract multiplicative pattern. Landahl [6] modified the

description of Table I by changing the dimensions and number of airways in some regions, and further subdividing the TB network to increase the total number of discrete regions. The Task Group on Lung Dynamics [1], while acknowledging the Findeisen [4] anatomical model to be "unsophisticated," considered it to be more physiologically realistic than the more elaborate descriptions and used it in their work.

Weibel [5] considered the Findeisen [4] TB description to be based on insufficient anatomical data, and termed the subdivision of the lung into nine compartments with different branching factors as "...entirely inadequate to represent the pulmonary architecture." Based upon morphological measurements, he proposed two models of the TB tree: one emphasizing its regular features (Model A), another emphasizing its irregularities (Model B). His anatomical measurements were made from a single cast of the major airways, and histological sectioning of lesser airways. Both have dichotomy as the fundamental branching pattern. The Model A is shown in Figure 2; a comparison with Figure 1 points out its simplicity of design. The lengths, diameters, and number of airways in each generation of the symmetric Model A are presented in Table II. The number of airways in each generation I, is 2^I; for example, there are 8,388,608 alveolar sacs. The architectural disparities between Tables I and II are pronounced.

Based upon airway measurements from a cast of a normal human lung, Horsfield et al. [7] proposed models which stress the asymmetric character of the lung. The models are not inclusive of alveolar ducts or sacs. The architectures were specifically defined so as to be suitable for use in physiologic calculations. The complexities of the

descriptions preclude a detailed discussion of them here. Suffice it to state that the descriptions utilize a dichotomous branching scheme and that a given generation is composed of airways of different "order" - that is, different dimensions. The correlation between Model 1 of Horsfield et al. [7] and Model A of Weibel [5] has been discussed (Martonen [8]).

Soong et al. [9] attempted to account for inter- and intrasubject variations in human lung structures by developing a probabilistic morphology. Using Weibel's [5] Model A as a foundation, they used its airway dimensions together with morphometric measurements of other investigators to establish statistical parameters to define airway length and diameter size distributions.

Perhaps the most ambitious attempt to quantitatively describe the lung structure of man and other mammalian species is that of Raabe et al. [10]. Morphometric measurements of airway lengths, diameters, branching angles, and gravity angles clearly revealed the variability of lung structure; indeed, to date, the sheer volume of data has limited their utilization in the modelling of lung functioning and aerosol deposition, etc. In an attempt to define a more simple, yet realistic, lung structure for use in studies of lung phenomena, Yeh and Schum [11] proposed a "Typical Path Lung Model" based upon the anatomical measurements. They utilized single typical pathways to represent either a portion of the lung such as a specific lobe, or the whole lung.

It is important to note that airways in a given array have the same physiological function (i.e., conducting airway, or gas exchange airway) in the Findeisen [4], Weibel Model A [5], Soong et al. [9], and Yeh and Schum [11] morphologies. This is not the case, however, in the

Horsfield et al. Model 1 [7] morphology. For example, there are 19 divisions from the trachea to the distal respiratory bronchioles in the Weibel Model A [5] description, but a range of 13-30 for Horsfield et al. [7] depending upon the pathway followed.

LUNG AIRFLOW PATTERNS

The nature (laminar or turbulent) of air flow within the lung is an important feature to be considered in modelling the behavior of inhaled aerosols. Moreover, knowledge of the nature of airstream velocity profiles in the lung is essential because they affect the trajectories, and subsequently the deposition probabilities, of particles. The subject has been well reviewed by Pedley et al., [12]. Here, we shall address only those factors which most significantly characterize airflow regimes within the lung.

The changing velocity profile of a viscous fluid as it flows through an idealized conduit (i.e., a straight, smooth, rigid-walled tube of circular cross-section and infinite length) is shown in Figure 3. A uniform, or flat, contour will eventually be transformed into a symmetric parabaloid shape because of the developing boundary layer at the fluid-wall interface. Under laminar flow conditions, a filament of dye injected into the fluid will retain its physical definition with passage through the conduit. When turbulent conditions exist, however, the filament will be disrupted and dye dispersed as illustrated in Figure 4. The final turbulent velocity profile will be a mean plug shape with superimposed random fluctuations. The fluid Reynolds number, Re, is a dimensionless parameter used to characterize fluid motion. For

an idealized conduit, it is defined as

$$Re = DU\upsilon^{-1}$$

where D is the tube diameter, and U and υ are the mean velocity and kinematic viscosity of the fluid, respectively. The transition from laminar to unstable motion may be considered to occur at about Re = 2300.

West and Hugh-Jones [13] studied flow patterns in large airways (trachea and main, lobar, and segmental bronchi) of a human replica lung cast. The cast was made using a transparent plastic material, and dye was injected into a stream of water flowing through it to visually discriminate between laminar and unstable conditions. Principles of dynamic similarity were used to determine air-equivalent flow conditions. At tracheal flow rates equivalent to 5 and 10 $Lmin^{-1}$ of air, motion was laminar in all airways. As flow increased, slight pertubations were first detected in the trachea (20 $Lmin^{-1}$), then unstable flows persisted through the main bronchi (40 $Lmin^{-1}$), and finally extended through the lobar bronchi (80 $Lmin^{-1}$). Important conclusions derived from the West and Hugh-Jones [13] data are:

- Since no laryngeal cast was present, the transition from laminar to unstable flows could be ascribed to anatomically faithful features of the TB cast, such as surface irregularities and airway branching.
- Airflow regimes in bronchial passages cannot be reliably predicted by fluid Reynolds number, Re, values. Its value was 1650 in the trachea at the flow rate of 20 $Lmin^{-1}$. Similarly, the unstable flows observed within main and lobar bronchi occurred at Re values significantly less than 2300.

Sekihara et al. [14] also investigated the transition from laminar to unstable flow in transparent replica casts of human upper bronchi without a larynx. The casts were pruned to consist of trachea to third, fourth, or fifth order bronchi. They calculated Re values based on a hydraulic diameter, D_h, where

$$D_h = \frac{4 \text{ (airway cross-sectional area)}}{\text{airway perimeter}}$$

to account for the nonuniform shape of bronchi. Unstable flow conditions were observed in the trachea at 15 $Lmin^{-1}$, as tracheal flow rates increased to 30 and 60 $Lmin^{-1}$ flow instabilities progressed through the main and lobar bronchi, respectively. At tracheal flow rates as large as 120 $Lmin^{-1}$, laminar conditions remained in fourth and fifth order bronchi. The data substantiated the West and Hugh-Jones [13] findings with regard to the disclosure that idealized tube Re values cannot always be used to estimate the nature of air flow in large bronchi.

The transition from laminar to unstable flow in replica human tracheal casts, with and without laryngeal casts, has been studied by Dekker [15]. He also utilized an injected dye-and-water system, and validated the extrapolation to air-equivalent flow conditions by performing a series of direct measurements on airflow through the casts with a hot wire anemometer. Without a laryngeal cast, the critical volumetric flow rate at which the transition took place was 21 $Lmin^{-1}$. The critical value was reduced to only 6 $Lmin^{-1}$ when laryngeal effects were included. Instabilities in the airstream, created upon movement through the narrow aperature of the glottis, are obviously quite

significant. (Note: Photographs of three replica laryngeal casts fixed at constant inspiratory flow rates of 15, 30 and 60 $Lmin^{-1}$ are shown in Figure 10.)

Schroter and Sudlow [16] and Sudlow et al. [17] studied air flow patterns in rigid plastic branched-tube models of one or two bifurcations based on dimensions of Weibel's Model A [5]. In the multiple bifurcation models, the second "Y" was either coplanar with the first or normal to it. The bifurcation angle was fixed at 70° after Horsfield and Cumming [18]. Inspiration and expiration were simulated, and flow profiles entering the models were either parabolic or flat. Their intent was to describe airstream behavior in subsegmental airways (i.e., generations 5-15). The authors considered the airflow regime within this region--from the location where upper airway turbulence has decayed to distal bronchioles where $1 < Re < 10$--to be "nominal laminar." During inspiration double vortex secondary currents were detected within sister airways; during expiration, a four vortex pattern was observed in the parent airway (see Figure 5). The primary velocity profiles within sister airways at locations downstream from a single bifurcation model during inspiration, as measured with a hot wire anemometer, are shown in Figure 6. The profiles were very asymmetric but stable, and flow characteristics were independent of Re and entry conditions. Testing with several models established that local geometry was the dominant factor affecting velocity profiles at bifurcation sites, namely, the curvature at the parent to daughter transition, and the shape of the carina, particularly as the latter affected separation of flow and flow reversal. Flow profiles downstream from a second bifurcation were not as asymmetric. On expiration, velocity profiles

downstream of a bifurcation were rather blunt and symmetric, probably due to impinging flows from sister airways.

Olson et al. [19] made replica casts of NP compartments and upper bronchi of cadavers and used them as molds to construct clear rubber models for use in fluid dynamics studies. The models were made of elastic, in an attempt to simulate actual airway deformations during breathing. Five laryngeal aperatures were made corresponding to constant flow rates ranging from 0.2 - 2.0 $Lmin^{-1}$. A hot wire anemometer was used to measure airstream velocities within an airway; indication of a mean velocity with a superimposed fluctuating component would signify turbulent conditions. Unstable flows were observed in all bronchi at all flow rates exceeding 0.2 $Lmin^{-1}$; that is, random fluctuations were present in sublobar bronchi even when $Re < 100$. The existence of turbulence at such small Re values was attributed to large scale disturbances created in upper bronchial flow fields following the onset at the laryngeal cast of a fluid dynamics phenomenon termed flow separation. Neither this study nor any of the aforementioned investigations addressed physiological factors such as pulsatile flow and cardiac pulsations which will certainly affect air flow patterns in vivo, although to what extent is not known.

EXPERIMENTAL AEROSOL DEPOSITION MODELS

To develop a laboratory model describing a physical process within the respiratory tract, such as aerosol deposition, one must first decide whether it is imperative that the model maintain the structural integrity (or, actual appearance) of the respiratory tract, or whether

it is sufficient for the model to mimic the specific process considered, in effect, permitting the respiratory tract *per se* to be a "black box". Here, we treat laboratory systems which attempt to simulate the actual branching network of the TB tree. We shall only comment that perhaps the best examples of "black box" instruments are the personnel dosimeters used for risk assessment of airborne particulate matter in workplace environments. Basically, the instruments separate sampled aerosols so that a "respirable" mass fraction--that penetrating to the alveolated portion of the lung--can be determined. Such devices include cyclones and mini-cascade impactors; the reader is directed to works such as Lippmann [20] and Martonen *et al*. [21] for references.

The primary aerosol deposition mechanisms in the respiratory tract are defined in Figure 7 where particulate behavior at a bronchial branching site is illustrated. Submicron-sized particles will exhibit random Brownian motion, and be deposited by diffusion. Larger particles will settle onto airway surfaces under the action of gravity; this deposition process is termed sedimentation. Other large particles possessing sufficient momentum will have paths deviating from curved fluid motion and be deposited by inertial impaction. The efficiencies of these mechanisms will be dependent upon local *in vivo* respiratory tract geometries and airstream characteristics--factors discussed earlier. Surrogate airway models used in studies intended to simulate inhaled aerosol behavior in man, therefore, must faithfully reproduce these factors.

Constant One-Way (i.e., Inspiration) Aerosol Motion

Laryngeal Simulator Absent

To determine the effect of particle size on the distribution of inhaled aerosols in man, Schlesinger and Lippmann [22] measured deposition patterns in three silicone rubber replica TB casts of the trachea (no larynx) through segmental bronchi. A spinning disc generator was used to produce monodisperse aerosols with mass median aerodynamic diameters (MMADs) ranging from 1.1-7.7 μm which were drawn through the casts at a constant 30 $Lmin^{-1}$ flow rate. The aerosols were ^{99m}Tc-labelled, and sites of deposition quantitated with a scintillation detector with a slit collimator. For similar particle sizes the total aerosol mass deposited within the TB casts varied greatly, supporting a hypothesis that differing airway morphology is a major cause of inter-subject variability in human test subject inhalation exposures. The relative dispersion of deposited material among TB airways, however, was similar. In most experiments deposition was enhanced at bronchial bifurcations; in one cast, for particles > 3.8 μm, ≅ 75% of the total aerosol mass deposited was found within the bifurcations.

Johnston et al. [23] and Johnston and Schroter [24] studied the deposition of monodisperse spinning disc-generated fluorescent aerosols in hand-fashioned Y-shaped airway units of dimensions comparable to Weibel Model A [5] generations 3-6. Bifurcation angles varied between 57-90°. Particle diameters ranged from 4.2-8.8 μm and laminar, steady parent flow rates had magnitudes of about 1-6 $Lmin^{-1}$. It was observed, but not quantitated, that aerosol was preferentially deposited at flow dividers (analogous to in vivo carina) within the bifurcation units. The authors presented an empirically-corrected modified-Landahl [6]

equation for deposition by inertial impaction, intended for use when airway bifurcation angles significantly exceed 60°.

Lee and Wang [25] measured the deposition of half-micron monodisperse triphenyl phosphate aerosols (condensation generator-produced) within two successive bifurcations, that is, three airway generations. The bifurcations were made from glass tubes and had dimensions corresponding to airway branchings situated at Weibel [5] Model A transitions from generations 2-3 and 3-4. Bifurcation angles were 64°. Two configurations were studied: (i) all bifurcations in the same plane, and (ii) second bifurcations normal to the first. Grids were placed along airway walls, and deposition determined with optical techniques. Aerosol flow was steady and laminar at 30 $Lmin^{-1}$. The effect of orientation was significant: in both cases deposition was enhanced at the carinal ridges within the second bifurcations, but in configuration (i) generation 4 airways had another "hot spot" that was ascribed to secondary flow patterns. The findings indicate the potential of aerosol maldistribution *in vivo* due to repeatedly bifurcating airways.

The dynamics of fluid motion within a clear plastic model of a human upper airway bifurcation has been studied by Schreck [26]. Using a miniature hot-wire anemometer, he measured skewed axial velocity distributions similar to those of Schroter and Sudlow [16]. Schreck [26] was able to correlate local variations in velocity gradients and convective transport with increased mass transfer of fluid at bifurcations, relative to other airway model wall locations.

Laryngeal Simulator Present

The incorporation of a replica laryngeal cast or surrogate in an experimental system improves the likelihood that downstream airflow patterns are similar to *in vivo* conditions. Ermala and Holsti [27] used a full-scale plaster model of the human oral cavity, larynx, trachea, and upper bronchi to study the deposition patterns of tobacco smoke. Deposition was enhanced at well defined locations ranging from the lips and vocal cords to bronchial bifurcations, and the localization of tobacco tar varied significantly depending on the type of smoking (pipe or cigarette) simulated.

From 1974-1978, members of the scientific staff of the Department of Environmental Medicine, New York University, conducted an extensive series of experimental studies-- *in vivo* and with models--with the objective of determining which factors most significantly affect inhaled particulate behavior in man. The *in vitro* efforts will be considered here. For the sake of brevity, common laboratory protocols are listed below prior to outlining major findings of the respective tests.

- ^{99m}Tc-labelled, nonhygroscopic, monodisperse aerosols were generated with a spinning disc instrument.
- A unique focusing collimator permitting high resolution of deposition patterns with great sensitivity was used.
- Replica silicone rubber laryngeal casts, molded from a cadaveric larynx with the glottic aperature fixed at constant inspiratory flow rates of 15, 30, and 60 $Lmin^{-1}$ were used. The multiple casts insured that air flow patterns within downstream bronchial passages were as physiologically realistic as possible, to date, to simulate.

- Replica silicone rubber TB casts were made from solid master casts of freshly excised human lungs, in some studies pruned to bronchioles no smaller than 2 mm in diameter. Typical casts are shown in Figure 8.
- The combined replica larynx-TB casts were contained within an artificial thorax during aerosol exposures.

The influences of the laryngeal jet and larynx-induced air flow instabilities on aerosol deposition in the trachea have been investigated by Schlesinger and Lippmann [28]. Aerosol particles ranged from 0.28-7 μm MMAD. Concentrated deposits were detected immediately distal to the laryngeal cast (within ≅ 2 cm) and could be attributed to direct impaction of large particles entrained in the laryngeal jet, and turbulent flow-related diffusion mechanisms for submicron particles. Intratracheal deposition patterns were more nonuniform than in the earlier [22] tests, and reported as being in closer agreement with *in vivo* measurements.

Investigations by Schlesinger *et al.* [29,30] have clearly demonstrated that aerosol deposition patterns within *in vitro* TB airways are very heterogeneous. The extent to which particles may be preferentially deposited at bronchial branching sites *in vivo* is shown in Table III. To represent the nonuniformity of deposition within a pair of sister bronchi, the tabulated values were computed by dividing the fraction of aerosol radioactivity found within the bifurcation by the respective surface area fraction; a value > 1 indicates enhanced deposition. The surface density distribution of particulate matter peaks at generation 3 bronchi, which correspond to *in vivo* segmental airways. In a comparable work (Schlesinger and Lippmann [31]), the

lobar bronchial bifurcations consistently received the most aerosol deposition.

Chan et al. [32] have quantitated the influence of electrostatic charge effects on particle deposition. Aerosol MMADs varied from about 2-7 μm. Total deposition of charged particles was enhanced significantly in the laryngeal and tracheal casts due to image forces, relative to like-sized aerosols that passed through an electric charge neutralizing device before entering the casts. The intensities of post-laryngeal cast "hot spots" in the trachea were about the same; the enhancement *per se* occurred primarily in midtracheal regions.

To determine if larynx-related flow phenomenon could influence particulate behavior in TB airways distal to the trachea, Lippmann and Altschuler [33] measured the deposition of a 9 μm MMAD aerosol in a TB cast at 45 $Lmin^{-1}$, with and without a laryngeal cast. Use of a laryngeal cast increased aerosol deposition in the surrogate trachea by a factor of ten. In the main, lobar, and segmental airways, however, deposition was greater in the TB cast that did not have a surrogate larynx placed upstream from it. The results suggest that the larynx will be an important anatomical feature affecting aerosol behavior *in vivo*. Using the same TB cast, they conducted a single experiment (aerosol MMAD = 6 μm, flow rate = 30 $Lmin^{-1}$) to ascertain the pattern of surface activity within bifurcations. The patterns were heterogeneous, and indicated that carinae were sites of concentrated deposits. The percent of total bifurcation deposition found at the carinae of main, lobar, segmental, and subsegmental bronchi of a replica TB cast ranged from 55%, 50-61%, 55-63%, to 32-80%, respectively.

Chan *et al.* [34] used a miniature hot wire anemometer to record velocity patterns and related the existence of turbulent air flow intensities to deposition "hot spots" in the trachea below laryngeal casts. The particles were in the 2.5-8 μm MMAD range. An empirical formula describing tracheal deposition as a function of an inertial impaction-related parameter, the particle Stokes number, St, was given as:

$$p(\tau) = 2.536\ St^{1.231}$$

where

$$St = \frac{\rho D^2 v}{18 \mu R} .$$

Parameters ρ and D are the density and geometric diameter of the particle, μ and v are the absolute viscosity and mean velocity of the airstream, and R is the radius of the trachea. The formula is valid for $St > 3 \times 10^{-3}$.

Ferron [35,36] used two glass models, constructed to approximate Weibel's [5] symmetric and asymmetric descriptions of the TB tree (Models A and B, respectively), to study factors affecting aerosol deposition. Each model consisted of six bronchial generations, and had a glass oropharyngeal compartment surrogate and laryngeal model--both of fixed geometry--placed upstream from it in laboratory tests. Experiments were conducted using constant flow rates, either 8 or 16 $Lmin^{-1}$, and polydisperse ^{99m}TC-labelled NaCl aerosols produced with jet nebulizers. The distributions of radioactivity within the TB models were determined with a NaI(T1) scintillation detector and collimators. The two aerosol sizes tested had MMADs and geometric standard deviations of about 0.88 μm and 2.05, and 1.69 μm and 1.89, respectively. In each test, about 50% of the total recorded activity was detected in the

oropharyngeal compartment surrogate; moreover, deposition was concentrated in the vicinity of its uvula component. Neither the total quantity of aerosol deposited, nor its intrabronchial distribution, varied appreciably between the two geometrically disimilar TB models.

The aforementioned deposition studies have produced data leading to a better understanding of the behavior of inhaled aerosols. Much remains to be done, however, and not all research institutions have access to human lungs to make replica casts, facilities to utilize radioactive materials, or technical and financial capabilities necessary to construct unique detection systems required to quantitate aerosol deposition. The need existed, therefore, for a TB model that could faithfully simulate in vivo airway morphology and fluid dynamics, and be expendable (i.e., be cut apart) to observe nonradioactive aerosol deposition patterns using common laboratory materials and instrumentation, such as fluorescent substances and spectrophotofluorometers, respectively. A single pathway TB model for use in aerosol studies has been proposed by Martonen and Lowe [35], Martonen [36], and Martonen and Hofmann [37]. An experimental system is shown in Figure 9. The hollow silicone rubber TB models were molded from a hand carved solid wax model made using Weibel's [5] upper bronchial airway dimensions. The bifurcation angle was 70° at all airway branching sites. Three silicone rubber laryngeal casts--with internal geometries appropriate for constant inspiratory flow rates of 15, 30 and 60 $Lmin^{-1}$--were molded from the original replica casts used in the previously discussed New York University Medical Center research program. The respective casts, together a schematic drawing of the laryngeal jet and larynx-promoted downstream airstream instabilities,

are illustrated in Figure 10. The rotameter arrangement in Figure 9 permitted aerosol flow through the combined laryngeal cast - TB model system to be precisely regulated. In the tests to be discussed, flows were split symmetrically at each airway branching.

The deposition patterns of monodisperse, spinning top - generated ammonium fluorescein aerosols at TB model bifurcations measured by Martonen and Lowe [37] and Martonen [38] are given in Table IV. The tabulated values follow the order of Table III; that is, generation 3 (segmental) bronchial bifurcations have the most aerosol mass deposited on a per-unit-area basis for each test, and generation 1, or main, bronchial bifurcations, the least. Data from these studies using single pathway TB models have also been demonstrated (Martonen [38]) to be the same as observed in the replica TB casts with regard to: total aerosol mass deposited, intrabronchial distribution of the total, and concentration of deposited particulate matter at carinal ridges.

The Martonen and Lowe [37] and Martonen [38] experiments also substantiated the results of earlier tests (Chan *et al.* [34]) which indicated that the larynx *in vivo* may quite effectively prevent appreciable quantities of large particles from penetrating to distal sites in the lung, particularly at high inspiratory flow rates. The fractional deposition probabilities of particles within the three laryngeal casts, $p(\ell)$, can accurately be expressed by the equation

$$p(\ell) = a + b\ St.$$

Slightly different values have been proposed for the constants a and b; Chan *et al.* [34] recommended 2.77×10^{-2} and 4.702, Martonen and Lowe [37] reported 3.5×10^{-2} and 3.9. In curve-fitting the laboratory data, St (see previous definition) was computed by assigning R a dimension of

1.65 cm, used to characterize the casts, and calculating v using laryngeal cast-specific cross-sectional areas of 0.88, 1.40 and 2.47 cm^2 (see Figure 10, panels A, B and C), respectively.

Recently, Martonen et al. [40] studied the distribution patterns of undiluted cigarette smoke in the three aforementioned laryngeal cast-single pathway TB model systems, now modified to include an oropharyngeal compartment. Deposition results for one of the cut apart TB models is schematically shown in Figure 11. The findings substantiated the Ermala and Holsti [27] observations of enhanced deposition occurring at bronchial bifurcations, and revealed two other heterogeneities: the nonuniformity of deposition at airway branching sites, i.e., the concentration of smoke particles at carinal ridges within bifurcations themselves, and the maldistribution of deposited cigarette smoke in bronchi. The latter pattern was shown to be in accordance with the action of the double vortex airstream currents seen in Figure 5.

Constant Two-Way (i.e., Inspiration and Expiration) Aerosol Motion Laryngeal Simulator Absent

Martin and Jacobi [41] examined the deposition of radiolabeled submicron (0.2-0.4 μm activity median diameter) aerosols in plastic TB models conforming to the first four generations of Weibel's [5] Model A morphology. Test aerosols were produced by the attachment of ^{212}Pb atoms to naturally occuring atmospheric particles. To compare aerosol deposition efficiencies during the inspiratory and expiratory phases of a simulated breathing cycle, two identical TB models were connected in series at the respective end bronchi. Aerosol motion, therefore, was from the trachea (I = 0) to segmental (I = 3) bronchi during inspiration,

and was reversed (I = 3 to I = 0) in the downstream model for expiration. Constant flow rates were varied from 0.1-50 $Lmin^{-1}$ in the tests. Neither a laryngeal cast nor surrogate was used in the tests. However, fortunately, the experimental arrangement was conducive to nonlaminar entry flow conditions in the trachea during inspiration. Autoradiographs showed that deposition was enhanced at airway bifurcations during inspiration and expiration. Indeed, particle deposition efficiences were almost independent of air flow direction: only for flow rates < 1 $Lmin^{-1}$ was deposition markedly greater during the simulated inspiratory phase of a breathing cycle. Measured deposition probabilities are in very good agreement with theoretical predictions assuming a nonlaminar flow field, indicating that turbulent diffusicn may be an important factor affecting aerosol behavior *in vivo*.

Laryngeal Simulator Present

Schlesinger *et al*. [42] used identical, silicone rubber replica TB casts, trachea through generation 4 bronchi, joined in series to compare particle deposition efficiencies at the same airway locations during inspiration and expiration. Monodisperse aerosols (^{99m}TC-labelled) were about 3-6 μm MMAD. The effects of constant flow rates of 15 and 30 $Lmin^{-1}$ were studied. An epoxy laryngeal cast, with a fixed opening of the glottis corresponding to a constant flow rate of 30 $Lmin^{-1}$ was placed upstream of the "inhalation" TB cast during all experiments. Aerosol deposition measurement data were normalized to the actual quantity of aerosol activity entering the respective casts. Deposition occurring during exhalation was a significant fraction of the two-cast total, ranging from 0.34-0.44. The intrabronchial distribution of

deposited particulate matter was quite different in the two casts: during inhalation deposition peaked at generation 3 airways in three out of the four conducted tests, while during expiration, deposition was favored at generation 1 and 2 airways (main and lobar bronchi *in vivo*). Preferential deposition took place at bronchial branching sites during exhalation as well as inhalation; indeed, the magnitude of that occurring during the former often exceeded the other. The locations of concentrated deposits, however, were not the same. For example, in the trachea-main bronchi transition during inspiration deposition was enhanced within the bifurcation *per se*; in the main bronchi-trachea transition during expiration deposition was enhanced in that portion of the trachea directly downstream (toward the larynx) of the bifurcation.

A similar pattern of "hot spots" occurring during inspiration and expiration was observed in tests using trachea-main bronchi sections of the aforementioned single pathway TB models connected in series. Monodisperse (7 μm MMAD) ammonium fluorescein aerosols were drawn at 30 $Lmin^{-1}$ through the two Y-shaped units. During inspiration, a laryngeal cast preceded the trachea. The deposition patterns are depicted in Figure 12. In panel A, concentrated deposits are seen at the carinal ridge, in panel B a highly localized deposit can be discerned in the trachea proper.

Pulsatile Aerosol Motion

Laryngeal Simulator Absent

Bell and Friedlander [43] and Bell [44,45] reported on the deposition of aerosols in two- and three-dimensional models, glass and metal, respectively, of the trachea-to-main bronchi bifuractions

constructed following Weibel's [5] Model A airway dimensions. The bifurcation angle was 70°. Monodisperse polystyrene particles with 0.088-7.6 μm diameters were sampled at steady and unsteady laminar flow conditions corresponding to time-averaged volumetric flowrates in the trachea of about 15 and 30 $Lmin^{-1}$. In both models, "No effort was made in these experiments to simulate actual conditions at the entry to the trachea[43]." Optical techniques were used to count particles deposited upon grids placed on model surfaces. Perhaps the most significant three-dimensional model findings were: (i) the discovery of peaks in particle transfer coefficients, or "hot spot" intensities, at the carina ranging from factors of 3.35-25.4 times greater than an integrated value over the whole airway surface (i.e., assuming uniform deposition); (ii) the detection of secondary peaks downstream from the carina; and, (iii) the determination that localized deposits of micron-sized particles at the carina were about five times more intense for pulsatile flows than steady flows of equal time-averaged flowrate.

The detailed analyses of localized aerosol deposition patterns were purportedly applicable to *in vivo* upper airways, where effects of the laryngeal jet and larynx-induced flow instabilities upon particle motion cannot be ignored. Moreover, particle deposition at carinal ridges will be affected by local airstream patterns. Chan *et al.* [34] used miniature hot-wire anemometers to map axial velocity profiles and turbulent intensities in a replica cast trachea-main bronchi bifurcation and the idealized bifurcation. The measurements indicate that the intense "hot-spots" of deposition detected by Bell [44,45] may be experimental artifacts of an aphysical transition geometry between the parent-daughter airways in the idealized model. It is not known to what

extent the absence of laryngeal casts or surrogates, and the unnatural bifurcation morphology, may have compromised the idealized bifurcation data.

The importance of accurately reproducing in vivo bifurcation geometries in surrogate models of bronchial airways to be used in aerosol experiments has been established by Haselton and Scherer [46]. They studied the effects of two-way pulsatile flows on the dispersion of neutrally bouyant, diffusion free 40 μm white beads in a multibranch five generation bronchial model. "Half airways" were routed out of two clear plastic sheets which were then clamped together to complete the model. The flow visualization experiments were conducted with glycerin as the fluid medium, and principles of dynamic similarity were used to simulate air flows in the in vivo lung corresponding to human bronchial generations 10-15. The differing velocity profiles generated at bifurcations during the inspiratory and expiratory phases of a breathing cycle were established as being the key factors affecting net particle and fluid flux across reference planes perpendicular to axial motion.

Laryngeal Simulator Present

Cheng and Wang [47] investigated the deposition patterns of 0.57-2.05 μm MMAD aerosols within a symmetric glass TB model (containing a fixed aperature larynx, trachea and four bronchial generations) under mean flow rate-equivalent steady and unsteady conditions. They measured local deposition velocities at second generation carinae oriented either co-planar with, or perpendicular to, the first generation airways. Deposition velocities were enhanced under unsteady conditions: the greatest difference, however, was only 26%--much less than the factor of 5 increase reported by Bell [44,45].

To simulate the effects of the larynx in aerosol deposition studies utilizing time-dependent air flow rates, Gurman et al. [48] developed a mechanical larynx with a variable "glottis" aperature. The unit mimics laryngeal airway changes, in both size and shape, that occur during a breathing cycle. It consists of two pivoted, rubber dam-covered metal strips whose pincer movement was controlled by a variable speed motor, drive gear, and cam. The cyclic movement of the strips through slots cut into a replica laryngeal cast was intended to simulate the action of the vocal cords in vivo.

Schlesinger et al. [49] used the aforementioned variable-opening replica laryngeal cast to study aerosol behavior in a replica TB cast obtained from the same autopsy specimen. The objective of the experiments was to quantitate the effects of constant versus cyclic flow patterns of equivalent mean flow rates of about 15, 30 and 60 $Lmin^{-1}$. Monodisperse, spinning disc-generated, ^{99m}Tc-tagged iron oxide aerosols had MMADs of either 3 or 8 μm. For similar particle Stokes numbers, deposition efficiences were greater under cyclic flow conditions regarding total activity measured within the cast. The intrabronchial distribution of deposited material, however, was the same. The differences between cyclic and constant flows were greatest for the smaller (3 μm MMAD) aerosols. These findings were attributed to: enhanced (relative to constant flows of like magnitude) turbulence in airways with cyclic flows, and a particle size-related deposition efficiency mechanism from a turbulent airstream onto a rough walled tube. The surface distribution of deposited particles within the trachea-main bronchi bifurcation was quantitated for the 8 μm MMAD aerosol under the cyclic and constant 15 and 60 $Lmin^{-1}$ flow rates. The

results are shown in Figure 13, panels A-D. Relatively, the most concentrated carinal ridge deposits were detected under constant flow conditions; particularly at the lowest flow rate (panel A).

DISCUSSION

Most experimental studies of aerosol behavior have focused upon factors influencing aerosol deposition in bronchial airways such as particle size and respiratory parameters. For ease of construction, most studies have used model systems constructed utilizing the simplest proposed bronchial morphology: Weibel's [5] symmetric Model A. As has been noted, there are several asymmetric TB geometries available for construction of physical models for use in investigating the effects of heterogeneous bronchial architecture on particle deposition. (Note: To date, these asymmetric descriptions have been limited to consideration in a few predictive aerosol deposition models; for example, Task Group on Lung Dynamics [1], Martonen [8], and Yeh and Schum [11]).

The numerous experimental investigations cited in this review suggest that inhaled aerosols may be preferentially deposited at certain respiratory tract sites *in vivo*. Regarding their qualitative, mapping studies of tobacco smoke deposition, Ermala and Host [27] wrote: "A striking correlation was noted between the clinical incidence of cancer and the localization of tobacco smoke." This was true for regions of the extrathoracic compartment such as the lips, tongue, cheek mucosa, tonsillar area and vocal cords, and downstream TB bifurcations. The qualitative work of Martonen *et al*. [39] has confirmed these earlier findings.

Schlesinger et al. [30] have demonstrated that replica casts of the TB tree are suitable surrogates for studying factors that influence aerosol deposition in vivo. It has been shown that properly constructed TB models may be used in lieu of such casts (Martonen [38]). Clinical observations of the frequency of ocurrence of carcinogenic tumors in lungs of man are in accord with the quantitative in vitro data of Tables III and IV which enumerate enhanced deposition "hot spots" within certain bronchial bifurcations; that is, carcinomas are found predominantly at lobar and segmental bronchi in human lungs (Garland et al., [50]; Sabour et al., [51]; Veeze, [52]). The Martin and Jacobi [41] and Schlesinger et al. [42] experiments suggest that the exposure of airway cells at branching sites to toxic substances may be exacerbated by the formation of additional "hot spots" during expiration.

In Figure 14, the relative distribution of total lobar bronchi activity measured in the Schlesinger and Lippmann [31] aerosol deposition experiments are shown. The patterns of deposition are independent of particle size and inspiratory flow rate. Since breathing parameters vary among a population and airborne contaminants differ in size, one may presuppose a similar pattern for site selectivity of lobar carcinomas if sites of initial deposition are related to cancer induction. Clinically documented data relating each of the lobar bronchi as sites of origin of primary carcinomas is also plotted in Figure 14. The observed correlation of data suggest a relationship between locations of aerosol deposition in vivo and lung cancer.

The importance of the quantitative in vitro detection of concentrated carinal ridge deposits over a wide range of steady and

pulsatile flows (Lippmann and Altschuler [33], and Schlesinger et al. [49]) in the etiology of lung cancer may be indicated by the findings of Kotin and Falk [53] and Auerbach et al. [54] which identify the prominance of neoplastic and preneoplastic lesions at bifurcations. Epithelial cells located at such sites will receive the greatest exposures to toxic agents following inhalation of airborne contaminants.

Ferron [36] compared his experimental data with predicted deposition patterns from a mathematical deposition model and stated that best agreement between theory and experiment could be found if "...it was concluded that the mean deposition by impaction has a minor influence on the deposition in a bifurcation."; which is to say, agreement was best when the calculated contribution by impaction was ignored, and only sedimentation and diffusion were considered. This observation, however, is not compatible with the data from other investigators, previously discussed, which quantitate the heterodispersity of deposition for comparable particle sizes and flow rates due to enhanced deposition at bifurcations from the inertial impaction mechanism. Hence, it seems likely that either the theory is incorrect, or that the assumption of a homogeneous distribution of deposited aerosol (made in the laboratory protocol to measure deposition per cm of glass model) produced artifacts in the data such that agreement between theory and experiment was only possible by ignoring impaction.

The laryngeal casts' deposition efficiencies measured by Martonen and Lowe [37] imply that the larynx in vivo may be a "hot spot" or site of selective deposition. Interestingly, in a recent clinical study of aerosol deposition in healthy subjects and patients with laryngeal

carcinomas (Stahlhofen [55]), it was reported that: intersubject variability with regard to laryngeal morphology was the most significant factor affecting the deposition of inhaled particles and subsequent susceptibility to cancer induction, and laryngeal deposition was enhanced greatly following the surgical removal of malignant tumors of the larynx.

The Chan et al. [32] data demonstrate the importance of using an aerosol electric charge neutralizer for in vitro and in vivo deposition studies to reduce experimental artifacts. The data also indicate the necessity to account for electric charge-induced effects on deposition in the hazard evaluation of airborne particulate matter found in the ambient environment and workplace atmospheres.

The experimental findings of Shreck [26] indicate that gaseous pollutants of health effects concern, such as ozone and NO_x compounds may also be concentrated at carinae in upper bronchi in vivo because of increased effectiveness of convective transport due to asymmetric fluid velocity profiles within bifurcations. If so, it may be prudent to account for such effects in dosimetry models considering the uptake of reactive gases from inhaled air, especially if uptake is gas-phase limited. Also, the findings of Haselton and Scherer [46] have indicated that the shapes of bronchial branching sites may be very important anatomical features affecting the rates of transfer of inhaled particles and gases within the lung, indicating the necessity of making physiologically realistic laboratory models for use in studies of aerosol behavior.

Since the Bell and Friedlander [43] and Bell [44,45] TB models had an aphysical bifurcation geometry, and did not utilize a laryngeal cast

or surrogate, it is not clear to what extent the findings of those aerosol deposition studies are applicable to human airways *in vivo*--particularly to the upper bronchi immediately distal to the larynx. It is advised, therefore, to exercise caution in utilizing such data for the risk assessment of inhaled particles.

In conclusion, heterogeneity of deposition has been detected in *in vitro* experiments over a wide range of particulate sizes and flow rate magnitudes--in a variety of surrogate larynx-TB models, for both constant and time-dependent flow patterns, and for both phases (inspiration and expiration) of a breathing cycle. It seems likely, therefore, that the findings will cover the spectrum of inhaled aerosol deposition variability among a population that could be ascribed to intersubject variability in respiratory tract architecture and breathing parameters. Hence, it is suggested that aerosol maldistribution in the human respiratory tract is an important element to be incorporated into future hazard assessment analyses of pollutant aerosols in the ambient and occupational environments.

REFERENCES

1. Task Group on Lung Dynamics. "Deposition and Retention Models for Internal Dosimetry of the Human Respiratory Tract," Health Phys. 12:173-207 (1966).

2. Hatch, T. and P. Gross. Pulmonary Deposition and Retention of Inhaled Particles (New York: Academic Press, 1964).

3. Raabe, O. G. "Deposition and Clearance of Inhaled Aerosols," in Mechanisms in Respiratory Toxicology, H. Witchi and P. Nettesheim, Eds. (Boca Raton, FL: CRC Press, 1982), pp. 27-76.

4. Findeisen, W. "Über das Absetzen Kliner, in der Luft Suspendierter Teilchen in der Menschlichen Lunge bei der Atmung," Pfluegers Arch. Ges. Physiol. 236:367-379 (1935).

5. Weibel, E. R. Morphometry of the Human Lung (Heidelberg: Springer-Verlag, 1963).

6. Landahl, H. D. "On the Removal of Air-Borne Droplets by the Human Respiratory Tract: I. The Lung," Bull. Math. Biophys. 12:43-56 (1950).

7. Horsfield, K., G. Dart, D. E. Olson, G. F. Filley and G. Cumming. "Models of the Human Bronchial Tree," J. Appl. Physiol. 31:207-217 (1971).

8. Martonen, T. B. "On the Fate of Inhaled Particles in the Human: A Comparison of Experimental Data with Theoretical Computations Based on a Symmetric and Asymmetric Lung," Bull. Math. Biol. 45:409-424 (1983).

9. Soong, T. T., P. Nicolaides, C. P. Yu and S. C. Soong. "A Statistical Description of the Human Tracheobronchial Tree Geometry," Respir. Physiol. 37:161-172 (1979).

10. Raabe, O. G., H. C. Yeh, G. M. Schum and R. F. Phalen. "Tracheobronchial Geometry: Human, Dog, Rat, Hamster," LF-53, Lovelace Foundation, Albuquerque, NM (1976).

11. Yeh, H. C., and G. M. Schum. "Models of Human Lung Airways and their Application to Inhaled Particle Deposition," Bull. Math. Bio., 42:461-480 (1980).

12. Pedley, T. J., R. C. Schroter and M. F. Sudlow. "Gas Flow and Mixing in the Airways," in Lung Biology in Health and Disease, Vol. 3, Bioengineering Aspects of the Lung, J. B. West, Ed. (New York: Marcell Dekker, Inc., 1977), pp. 163-265.

13. West, J. B., and P. Hugh-Jones. "Patterns of Gas Flow in the Upper Bronchial Tree," J. Appl. Physiol. 14:753-759 (1959).

14. Sekihara, T., D. E. Olson and G. F. Filley. "Airflow Regimes and Geometrical Factors in the Human Airway," in Proceedings of Eleventh Aspen Emphysema Conference (Arlington, VA: US Dept. of Health, Education, and Welfare, 1968), pp. 103-114.

15. Dekker, E. "Transition Between Laminar and Turbulent Flow in Human Trachea," J. Appl. Physiol. 16:1060-1064 (1961).

16. Schroter, R. C., and M. F. Sudlow. "Flow Patterns in Models of the Human Bronchial Airways," Resp. Physiol. 7:341-355 (1969).

17. Sudlow, M. F., D. E. Olson and R. C. Schroter. "Fluid Mechanics of Bronchial Air-Flow," in Inhaled Particles III (London: Allen and Unwin Ltd., 1970), pp. 19-31.

18. Horsfield, K., and G. Cumming. "Angles of Branching and Diameters of Branches in the Human Bronchial Tree," Bull. Math. Biophys. 29:245-259 (1967).

19. Olson, D. E., M. F. Sudlow, K. Horsfield and G. F. Filley. "Convective Patterns of Flow During Inspiration," Arch. Intern. Med. 131:51-57 (1973).

20. Lippmann, M. "'Respirable' Dust Sampling," in Air Sampling Instruments for Evaluation of Atmospheric Contaminants, 5th Edition, (Cincinnati, OH: ACGIH, 1978), pp. G1-G23.

21. Martonen, T. B., M. Clark, D. Nelson, E. Rossignol and D. Willard. "Testing of Personnel Dosimetry Devices for Hazard Evaluation of Solvent Refined Coal Droplet Aerosols," Am. Ind. Hyg. Assoc. J. 44:52-54 (1983).

22. Schlesinger, R. B., and M. Lippmann. "Particle Deposition in Casts of the Human Upper Tracheobronchial Tree," Am. Ind. Hyg. Assoc. J. 33:237-251 (1972).

23. Johnston, J. R., K. D. Isles and D. C. F. Muir. "Inertial Deposition of Particles in Human Branching Airways," in Inhaled Particles IV, W. H. Walton, Ed. (Oxford: Pergamon Press, 1977), pp. 61-73.

24. Johnston, J. R., and R. C. Schroter. "Deposition of Particles in Model Airways," J. Appl. Physiol. 47:947-953 (1979).

25. Lee, W. C., and C. S. Wang. "Particle Deposition in Systems of Repeatedly Bifurcating Tubes," in Inhaled Particles IV, W. H. Walton, Ed. (Oxford: Pergamon Press, 1977), pp. 49-59.

26. Schreck, R. M. "Mass Transfer of Nitrogen Dioxide in Lung Airway Bifurcations," Research Publication GMR-4411, General Motors Research Laboratories, Warren, MI (1983).

27. Ermala, P., and L. R. Holsti. "Distribution and Absorption of Tobacco Tar in the Organs of the Respiratory Tract," Cancer 8:673-678 (1955).

28. Schlesinger, R. B., and M. Lippmann. "Particle Deposition in the Trachea: in vivo and in Hollow Casts," Thorax. 31:678-684 (1976).

29. Schlesinger, R. B., V. R. Cohen and M. Lippmann. "Studies of Intrabronchial Particle Deposition Using Hollow Bronchial Casts," in Experimental Lung Cancer: Carcinogenesis and Bioassays, E. Karbe and J. F. Park, Eds. (Heidelberg: Springer-Verlag, 1974), pp. 116-127.

30. Schlesinger, R. B., D. E. Bohning, T. L. Chan and M. Lippmann. "Particle Deposition in a Hollow Cast of the Human Tracheobronchial Tree," J. Aerosol. Sci. 8:429-445 (1977).

31. Schlesinger, R. B., and M. Lippmann. "Selective Particle Deposition and Bronchogenic Carcinoma," Environ. Res. 15:424-431 (1978).

32. Chan, T. L., M. Lippmann, V. R. Cohen and R. B. Schlesinger. "Effect of Electrostatic Charges on Particle Deposition in a Hollow Cast of the Human Larynx-Tracheobronchial Tree," J. Aerosol Sci. 9:463-468 (1978).

33. Lippmann, M., and B. Altshuler. "Regional Deposition of Aerosols," in Air Pollution and the Lung, E. F. Aharonson, A. Ben-David and M. A. Klingberg, Eds. (New York: John Wiley and Sons, Inc., 1976), pp. 25-48.

34. Chan, T. L., R. M. Schreck and M. Lippmann. "Effect of the Laryngeal Jet on Particle Deposition in the Human Trachea and Upper Bronchial Airways," J. Aerosol Sci. 11:447-459 (1980).

35. Ferron, G. A. "On the Deposition of Aerosols in the Human Airways," Ph.D. Thesis, Technische Hogeschool Delft, The Netherlands (1976).

36. Ferron, G. A. "Deposition of Polydisperse Aerosols in Two Glass Models Representing the Upper Human Airways," J. Aerosol. Sci. 8:409-427 (1977).

37. Martonen, T. B., and J. Lowe. "Assessment of Aerosol Deposition Patterns in Human Respiratory Tract Casts," in Aerosols in the Mining and Industrial Work Environments, Vol. 1, V. A. Marple and B. Y. H. Liu, Eds. (Ann Arbor, MI: Ann Arbor Science, 1983), pp. 151-163.

38. Martonen, T. B. "Measurement of Particle Dose Distribution in a Model of a Human Larynx and Tracheobronchial Tree," J. Aerosol Sci. 14:11-22 (1983).

39. Martonen, T. B., and W. Hofmann. "Experimental Studies of Aerosol Behavior in Human Respiratory Tract Models: Implications to Dosimetry," in J. Aerosol Sci. (Oxford: Pergamon Press, 1984), pp. 200-203.

40. Martonen, T. B., W. Hofmann and J. E. Lowe. "Cigarette Smoke and Lung Cancer," Health Phys. (in press).

41. Martin, D., and W. Jacobi. "Diffusion Deposition of Small-Sized Particles in the Bronchial Tree," Health Phys. 23:23-29 (1972).

42. Schlesinger, R. B., J. Concato and M. Lippmann. "Particle Deposition During Exhalation: a Study in Replicate Casts of the Human Upper Tracheobronchial Tree," in Aerosols in the Mining and Industrial Work Environments, Vol. 1, V. A. Marple and B. Y. H. Liu, Eds. (Ann Arbor, MI: Ann Arbor Science, 1983), pp. 165-176.

43. Bell, K. A., and S. K. Friedlander. "Aerosol Deposition in Models of a Human Lung Bifurcation," Staub-Reinhalt Luft 33:183-187 (1973).

44. Bell, K. A. "Aerosol Deposition in Models of aHuman Lung Bifurcation," Ph.D. Thesis, California Institute of Technology, Pasadena, CA, USA (1974).

45. Bell, K. A. "Local Particle Deposition in Respiratory Airway Models," in Recent Developments in Aerosol Science, D. T. Shaw, Ed. (New York: John Wiley and Sons, Inc., 1978), pp. 97-133.

46. Haselton, F. R., and P. W. Scherer. "Bronchial Bifurcations and Respiratory Mass Transport," Science 208:69-71 (1980).

47. Cheng, J., and C. Wang. "Particle Deposition from Simulated Respiratory Flows in a Bronchial Tree Model," paper presented at the American Industrial Hygiene Conference, Atlanta, GA, May 16-21, 1976.

48. Gurman, J. L., R. B. Schlesinger and M. Lippmann. "A Variable-Opening Mechanical Larynx for Use in Aerosol Deposition Studies," Am. Ind. Hyg. Assoc. J. 41:678-680 (1980).

49. Schlesinger, R. B., J. L. Gurman and M. Lippmann. "Particle Deposition within Bronchial Airways: Comparisons Using Constant and Cyclic Inspiratory Flows," Ann. occup. Hyg. 26:47-64 (1982).

50. Garland, L. H., R. L. Beier, W. Colson, J. H. Heald and R. L. Stein. "The Apparent Sites of Origin of Carcinomas of the Lung," Radiology 78:1-11 (1962).

51. Sabour, M. S., L. M. Osman, J. Glen, T. Fahy and P. Lamb. "Carcinoma of the Lung. Review of 509 Cases," Dis. Chest 41:530-546 (1962).

52. Veeze, P. Rationale and Methods of Early Detection in Lung Cancer (Assen: Van Gorcum and Co., 1968).

53. Kotin, P., and H. L. Falk. "The Role and Action of Environmental Agents in the Pathogenesis of Lung Cancer. I. Air Pollutants," Cancer 12:147-163 (1959).

54. Auerbach, O., A. P. Stout, E. C. Hammond and L. Garfinkel. "Changes in Bronchial Epithelium in Relation to Cigarette Smoking and in Relation to Lung Cancer," N. Engl. J. Med. 265:253-267 (1961).

55. Stahlhofen, W., J. Gebhart, J. Heyder, G. Scheuch and P. Juraske. "Particle Deposition in Extrathoracic Airways of Healthy Subjects and of Patients with Early Stages of Laryngeal Carcinoma," in J. Aerosol Sci. (Oxford: Pergamon Press, 1984), pp. 215-217.

Table I. Architecture of the Human Lung Proposed by Findeisen [4]

Anatomical Region	Airway Diameter (cm)	Airway Length (cm)	Airway Number
trachea	1.3	11	1
1st order bronchi	0.75	6.5	2
2nd order bronchi	0.4	3.0	12
3rd order bronchi	0.2	1.5	100
4th order bronchi	0.15	0.5	770
terminal bronchioles	0.06	0.3	5.4×10^4
respiratory bronchioles	0.05	0.15	1.1×10^5
alveolar ducts	0.02	0.02	2.6×10^7
alveolar sacs	0.03	0.03	5.2×10^7

Table II. Anatomical Description of Weibel's [5] Model A Lung Architecture.*

Airway Generation (I)	Anatomical Site	Airway Diameter (cm)	Airway Length (cm)
0	trachea	1.8	12.0
1	main bronchi	1.22	4.76
2	lobar bronchi	0.83	1.90
3	segmental bronchi	0.56	0.76
4	subsegmental bronchi	0.45	1.27
5	"	0.35	1.07
6	"	0.28	0.90
7	"	0.23	0.76
8	"	0.186	0.64
9	"	0.154	0.54
10	"	0.130	0.46
11	"	0.109	0.39
12	"	0.095	0.33
13	"	0.082	0.27
14	"	0.074	0.23
15	"	0.066	0.20
16	terminal bronchioles	0.060	0.165
17	respiratory bronchioles	0.054	0.141
18	"	0.050	0.117
19	"	0.047	0.099
20	alveolar ducts	0.045	0.083
21	"	0.043	0.070
22	"	0.041	0.059
23	alveolar sacs	0.041	0.050

*Dimensions relate to an adult lung with a total volume of 4800 cm^3 at 3/4 maximal inflation

Table III. Intrabronchial Distribution Patterns of Aerosols Deposited Among Replica Tracheobronchial Cast Bifurcations (from Schlesinger et al. [29,30])

Bifurcation Location (Generation) I	15* L min^{-1}							30 L min^{-1}			60 L min^{-1}					
	0.28§ µm	3.0 µm	3.1 µm	4.2 µm	4.4 µm	7.0 µm	7.1 µm	2.8 µm	5.2 µm	7.7 µm	2.5 µm	2.6 µm	4.4 µm	4.8 µm	8.0 µm	8.1 µm
1	0.47●	0.28	0.67	0.51	0.80	0.87	0.80	0.09	0.25	1.06	0.57	1.33	0.52	1.07	1.60	0.76
2	2.67	1.15	2.73	1.06	1.73	2.47	0.95	1.42	1.04	0.78	0.67	2.80	1.46	1.40	3.33	1.47
3	2.13	1.68	2.07	2.99	2.33	2.93	2.31	3.08	2.73	3.06	1.87	1.93	1.91	2.07	4.53	1.78
4	0.87	1.16	1.20	1.64	1.80	1.87	1.75	1.24	1.48	1.97	1.54	2.00	1.65	2.13	2.40	1.65
5	----†	1.06	----	1.09	----	----	1.00	1.11	1.05	1.37	1.12	----	1.98	----	----	1.20
6	----	0.77	----	0.99	----	----	1.03	1.17	1.05	1.10	1.34	----	1.27	----	----	0.98

* Constant inspiratory flow rate

§ Aerosol mass median aerodynamic diameter

● Data = (bifurcation deposition/total sister airway deposition, bifurcation inclusive) ÷ (bifurcation surface area/total sister airway surface area, bifurcation inclusive). Value > 1 indicates deposition enhancement.

† Cast inclusive of trachea-first generation of subsegmental bronchi

Table IV. Intrabronchial Distribution Patterns of Aerosols Deposited Among Single Pathway Tracheobronchial Model Bifurcations (from Martonen and Lowe [37]; and Martonen [38])

Bifurcation Location (Generation) I	15* L min^{-1}				30 L min^{-1}			60 L min^{-1}			
	1.9§ μm	2.1 μm	3.0 μm	6.7 μm	3.3 μm	3.6 μm	6.8 μm	1.9 μm	6.1 μm	8.7 μm	10.6 μm
1	0.80[a]	0.42	0.51	0.83	0.17	0.25	0.65	0.50	0.84	1.01	1.20
2	1.15	1.08	1.15	0.92	1.08	1.19	1.35	1.30	1.14	1.40	1.52
3	1.50	1.38	1.62	1.36	2.29	1.83	2.31	1.93	1.84	3.05	3.16
4	0.91	0.90	0.87	1.12	1.34	1.47	1.57	1.74	1.46	2.10	1.94
5	1.10	0.85	0.91	1.18	1.48	1.63	1.50	1.63	1.78	1.75	1.60

* Constant inspiratory flow rate

§ Aerosol mass median aerodynamic diameter

[a] Data = (bifurcation deposition/total sister airway deposition, bifurcation inclusive) ÷ (bifurcation surface area/total sister airway surface area, bifurcation inclusive). Value > 1 indicates deposition enhancement.

Figure 1. Illustration of the human respiratory tract with identification of key anatomical and physiological components. Insert shows a silicone rubber replica TB cast pruned to 3 mm diameter bronchioles, dissected distal segments inclusive of terminal bronchioles, and respiratory acinus bundles (from Hatch and Gross (2) and Raabe (3)).

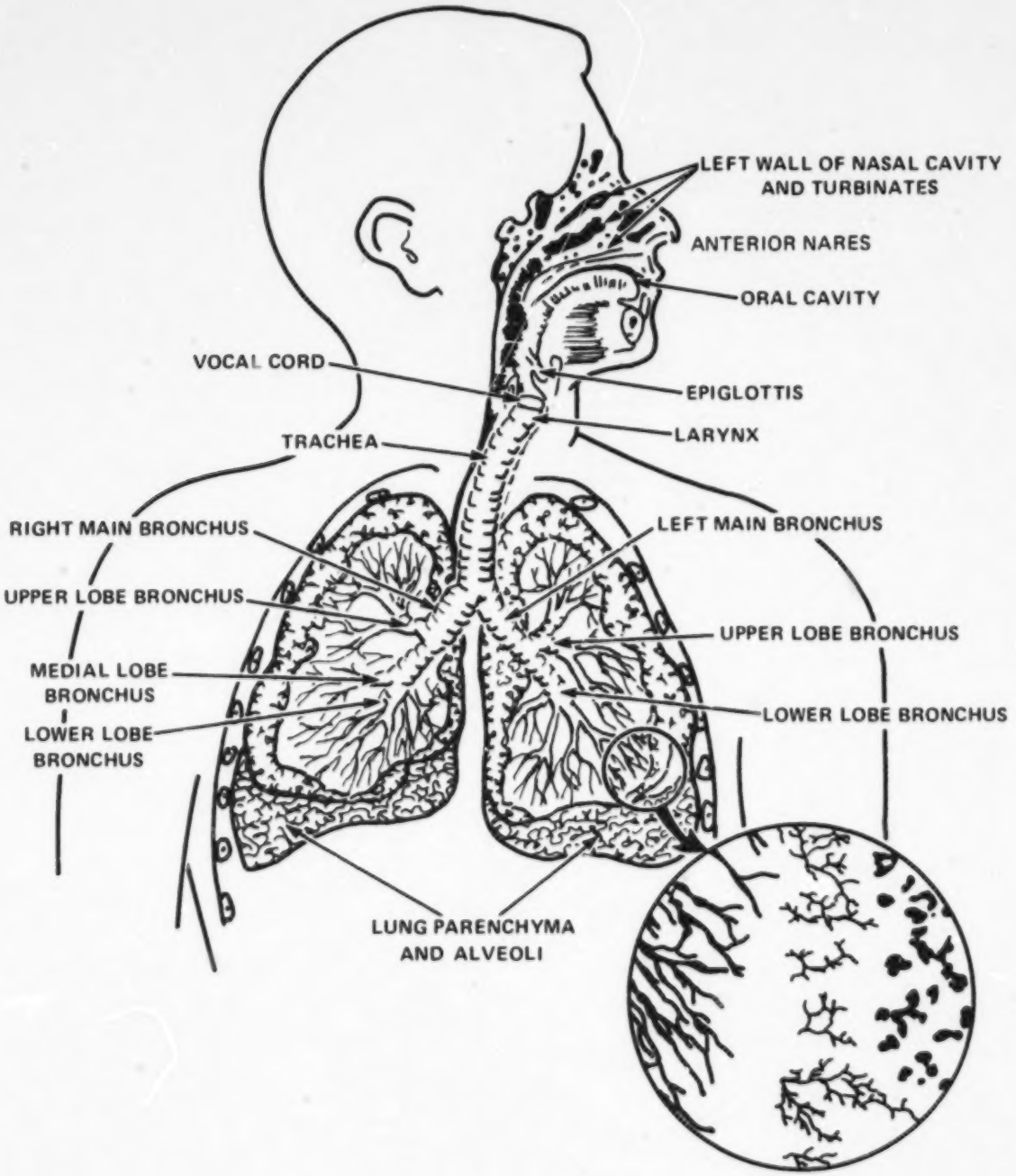

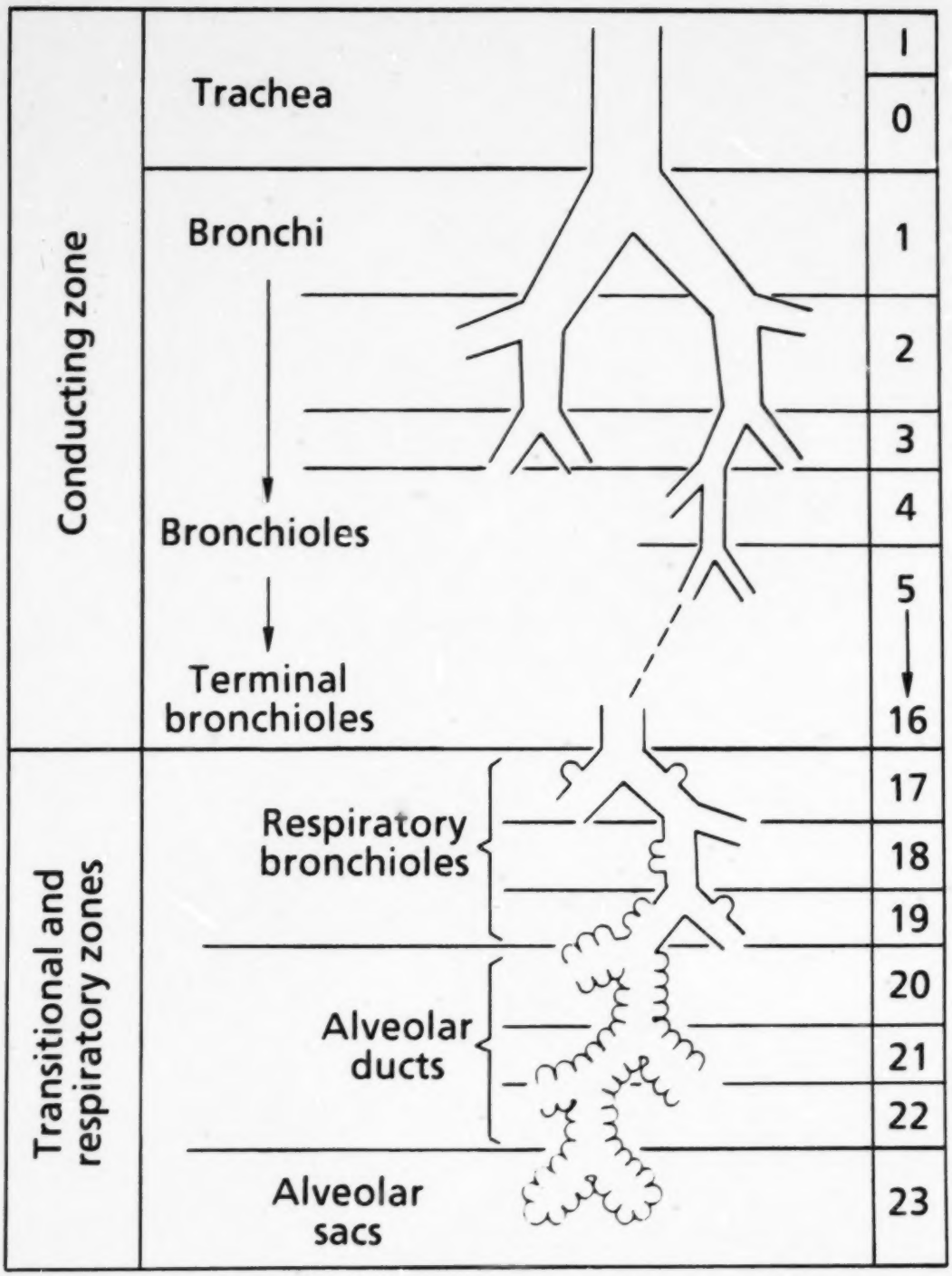

Figure 2. A description of the human lung assuming a symmetric, dichotomously branching morphology (from Weibel (5)).

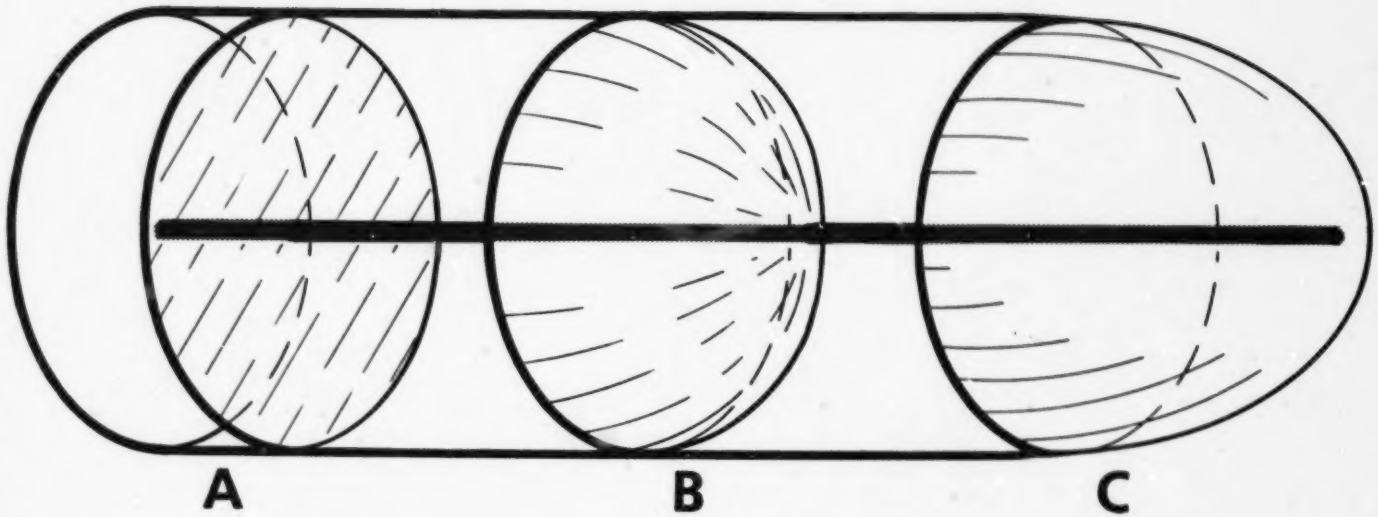

Figure 3. Transition of primary (axial) fluid velocity profiles in an idealized conduit under laminar conditions from (A) uniform flow, (B) transition contour, to (C) plug flow profile. Dissipated stream filament indicates turbulent flow.

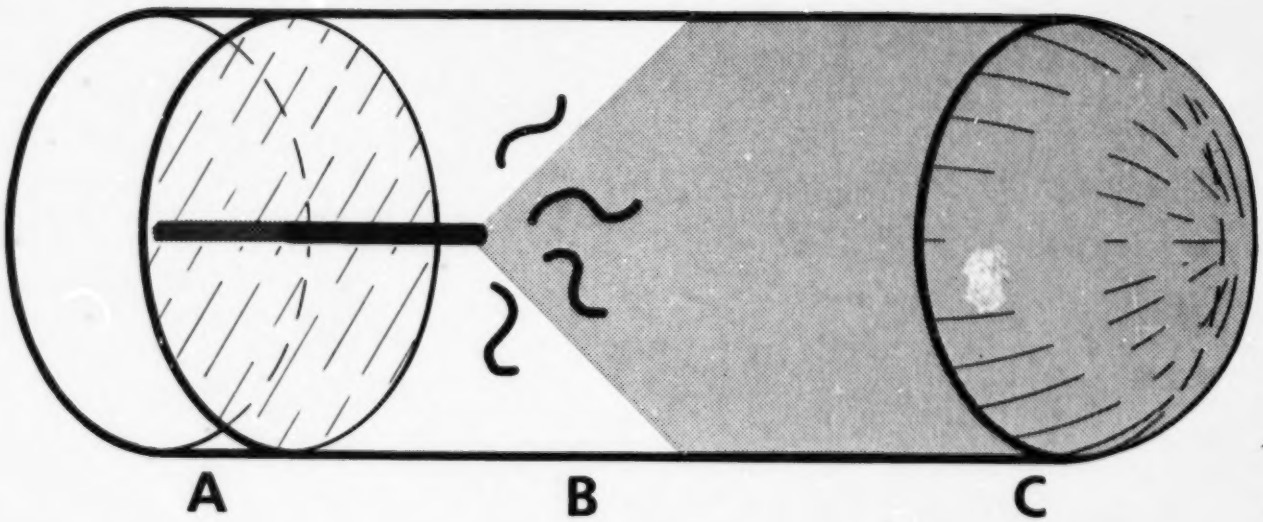

Figure 4. Transition of primary (axial) fluid velocity profiles in an idealized conduit under turbulent conditions from (A) uniform flow, (B) onset of turbulence, to (C) plug flow profile. Dissipated stream filament indicates turbulent flow.

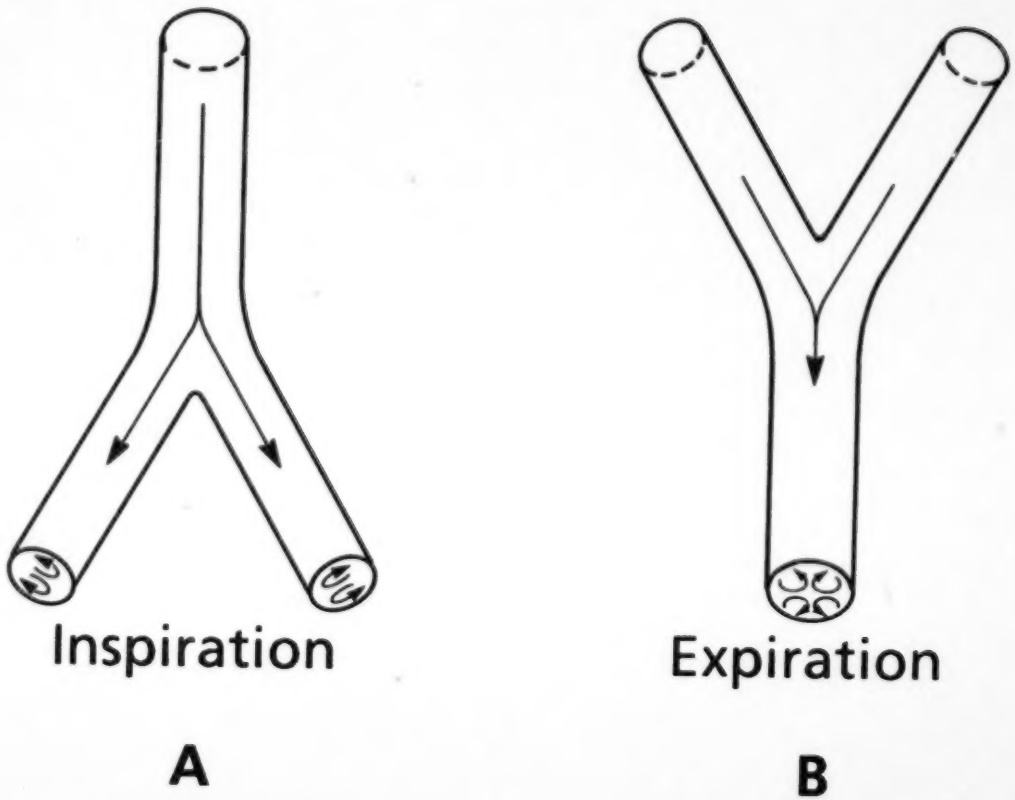

Figure 5. Secondary velocity currents occurring downstream of a bronchial branching site: (A) double vortex pattern during inspiration, (B) quadruple vortex pattern during expiration.

Figure 6. Axial fluid velocity profiles downstream of a bronchial branching site under laminar conditions: (A) in the plane perpendicular to the bifurcation, (B) in the plane of the bifurcation.

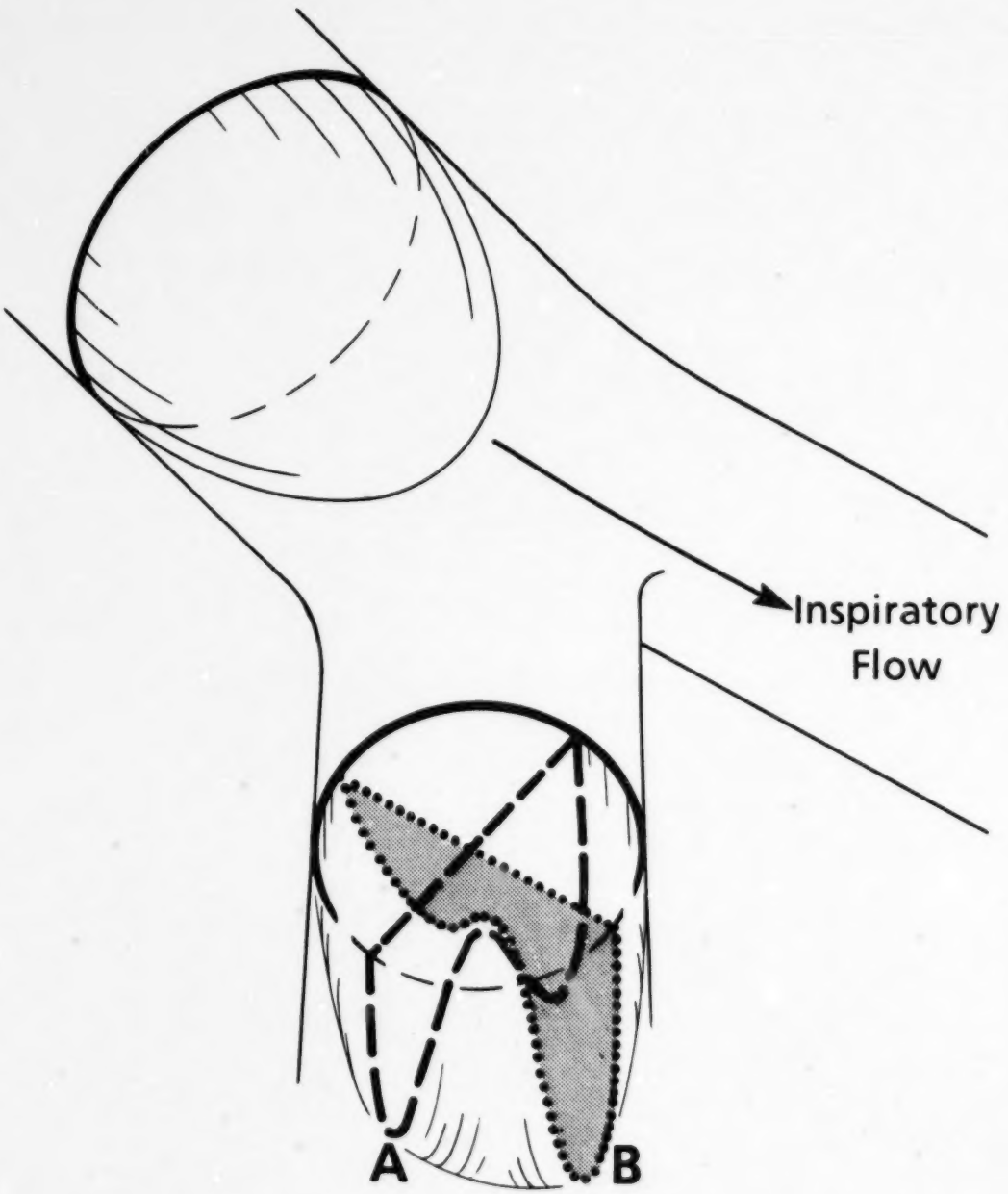

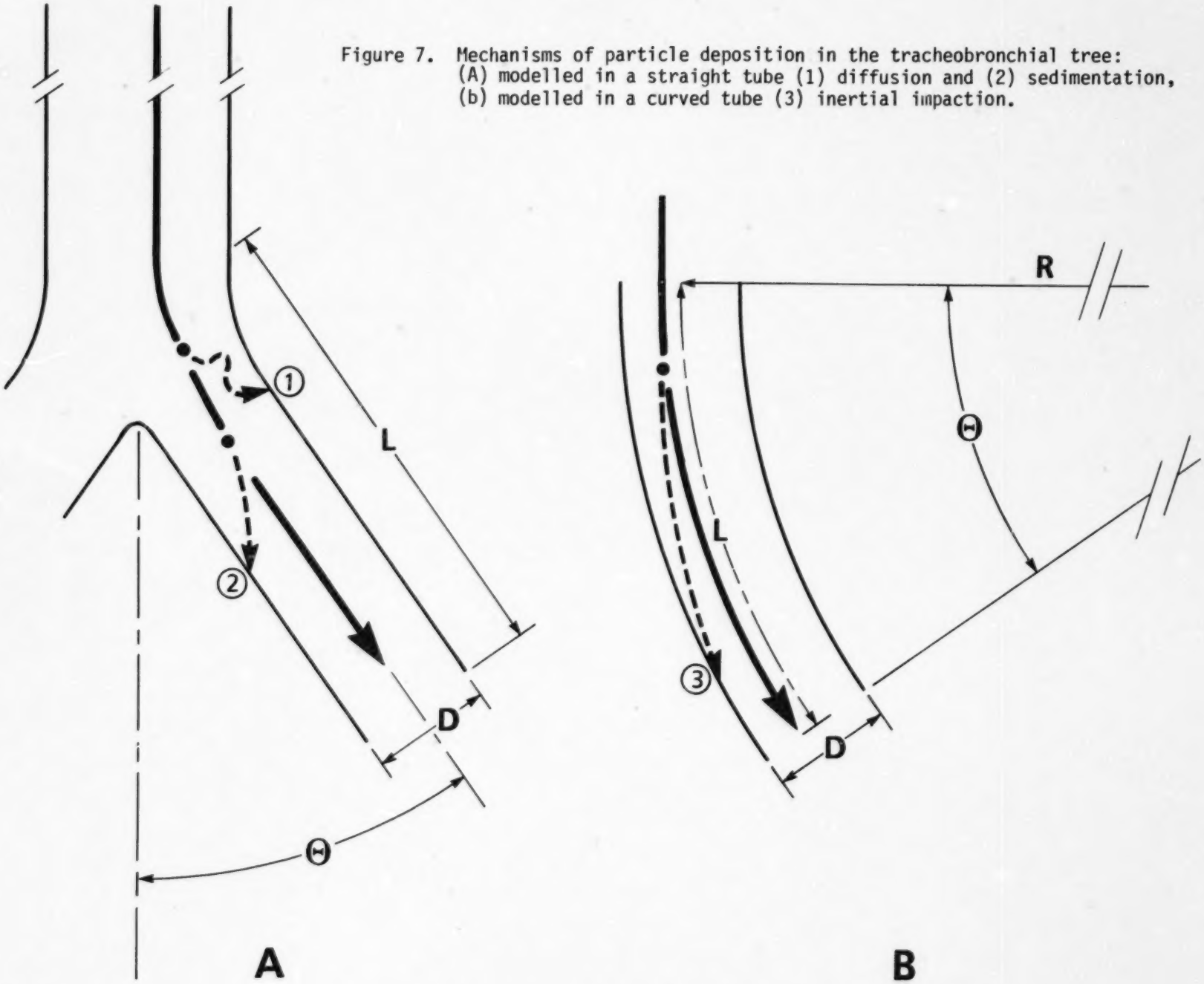

Figure 7. Mechanisms of particle deposition in the tracheobronchial tree: (A) modelled in a straight tube (1) diffusion and (2) sedimentation, (b) modelled in a curved tube (3) inertial impaction.

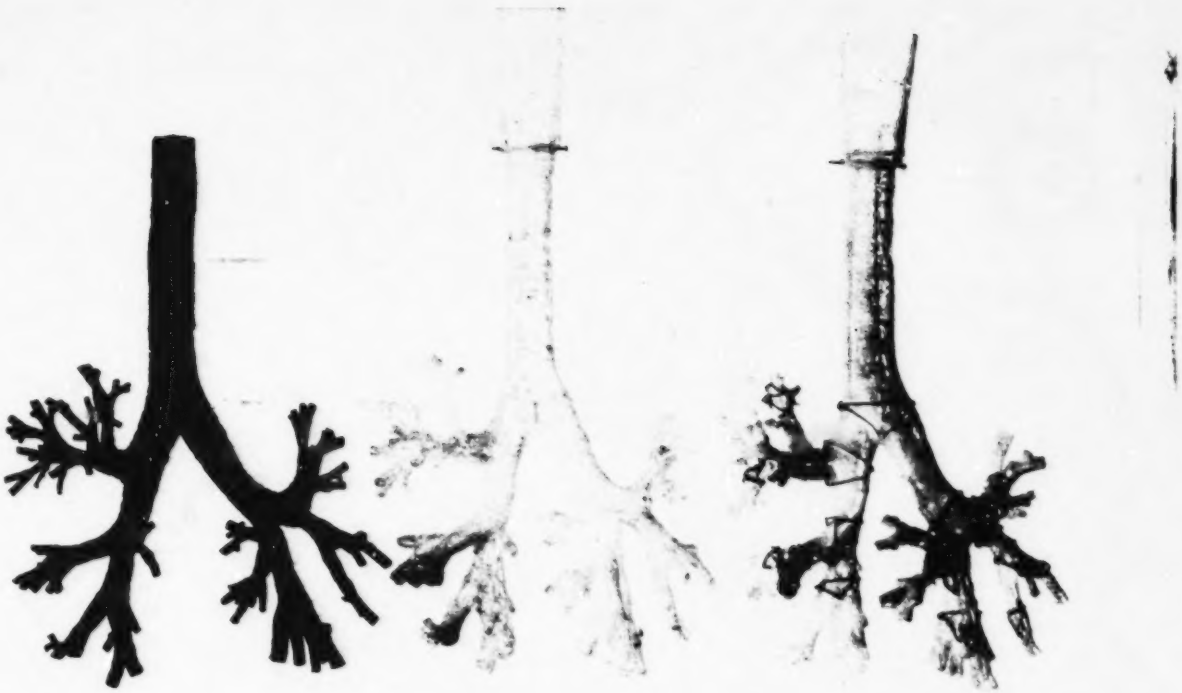

Figure 8. Silicone rubber replica casts of upper airways of the human tracheobronchial tree. Fron left to right: solid master cast, hollow cast, and hollow cast marked off for aerosol depositon tests (from Schleisinger et al. (49)).

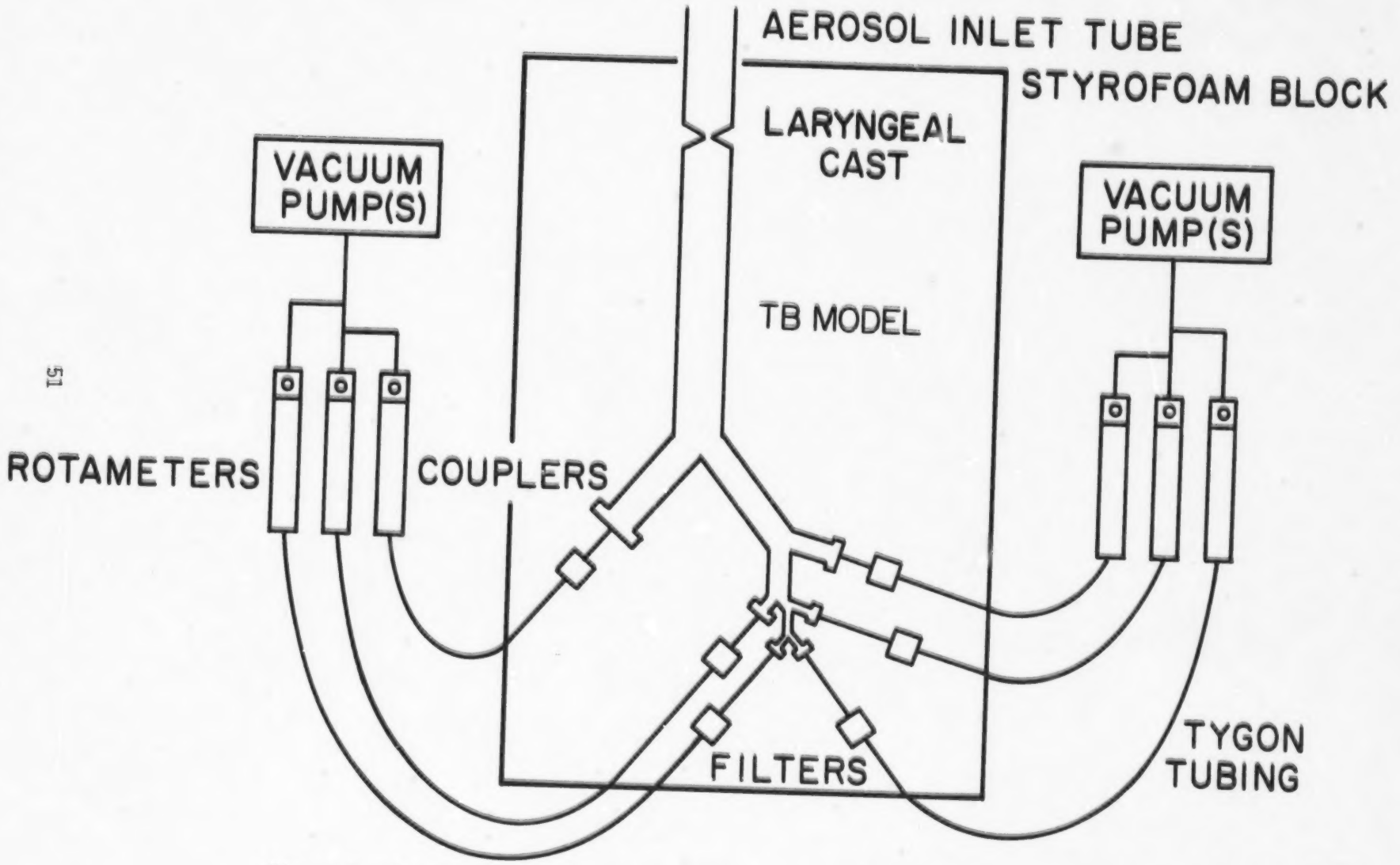

Figure 9. Surrogate experimental system consisting of a single pathway tracheobronchial model and replica laryngeal cast used to study aerosol behavior in man (from Martonen (38)).

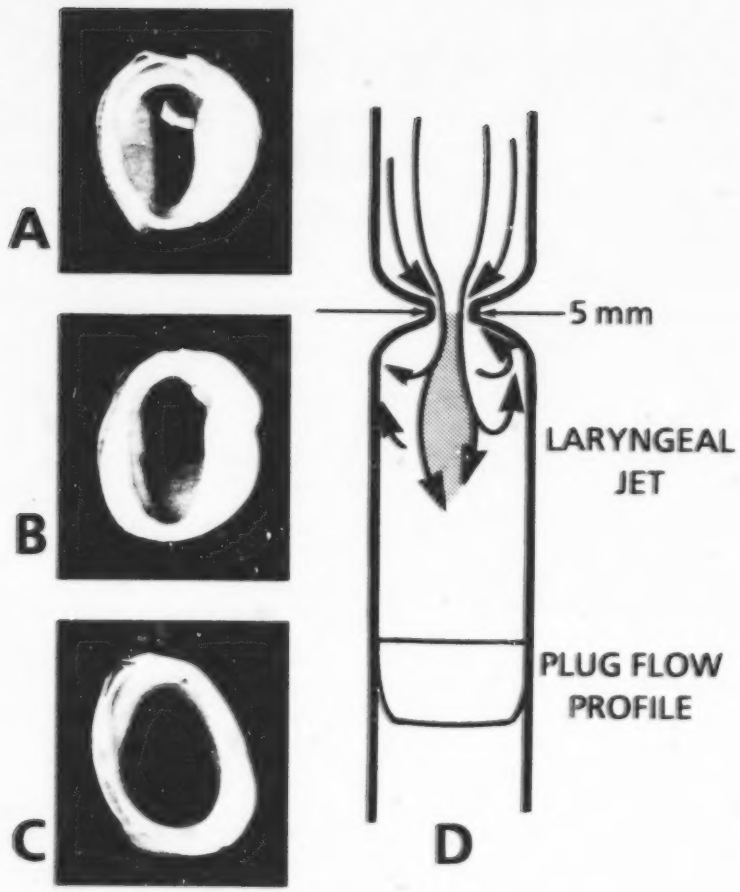

Figure 10. Geometry of the larynx as a function of inspiratory flow rate, and effect of the larynx on airstream dynamics. Replica cast aperatures of the glottis correspond to (A) 15, (B) 30, and (C) 60 $Lmin^{-1}$, respectively. Laryngeal jet and flow instabilities shown in (D).

Figure 11. Graphic artist's representation of the distribution of deposited cigarette smoke particles within a single pathway TB model (from Martonen et al. (40)).

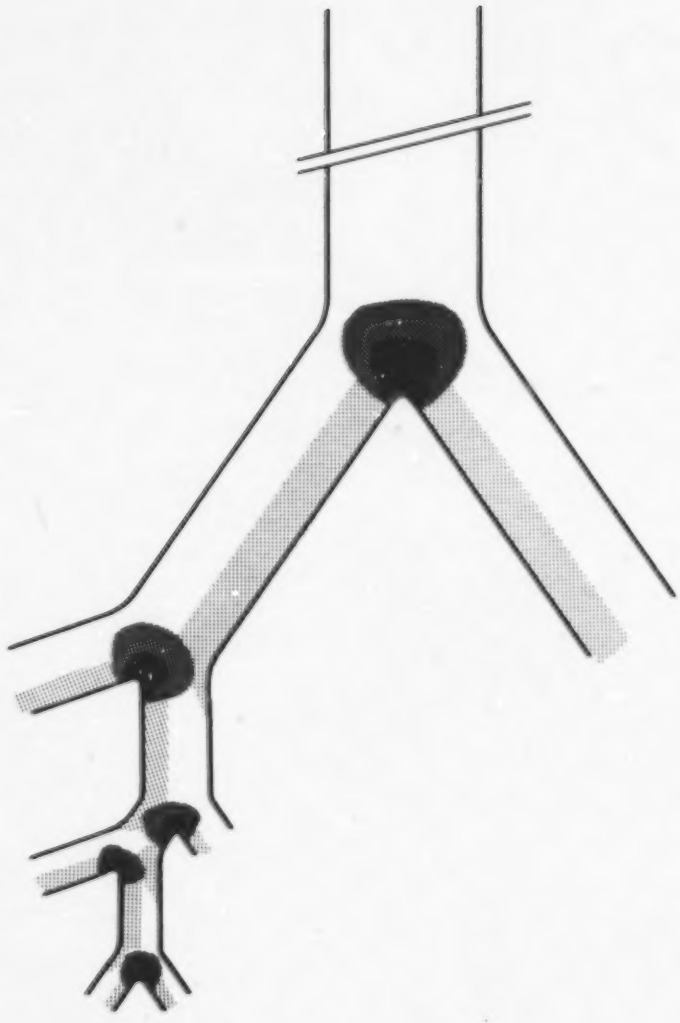

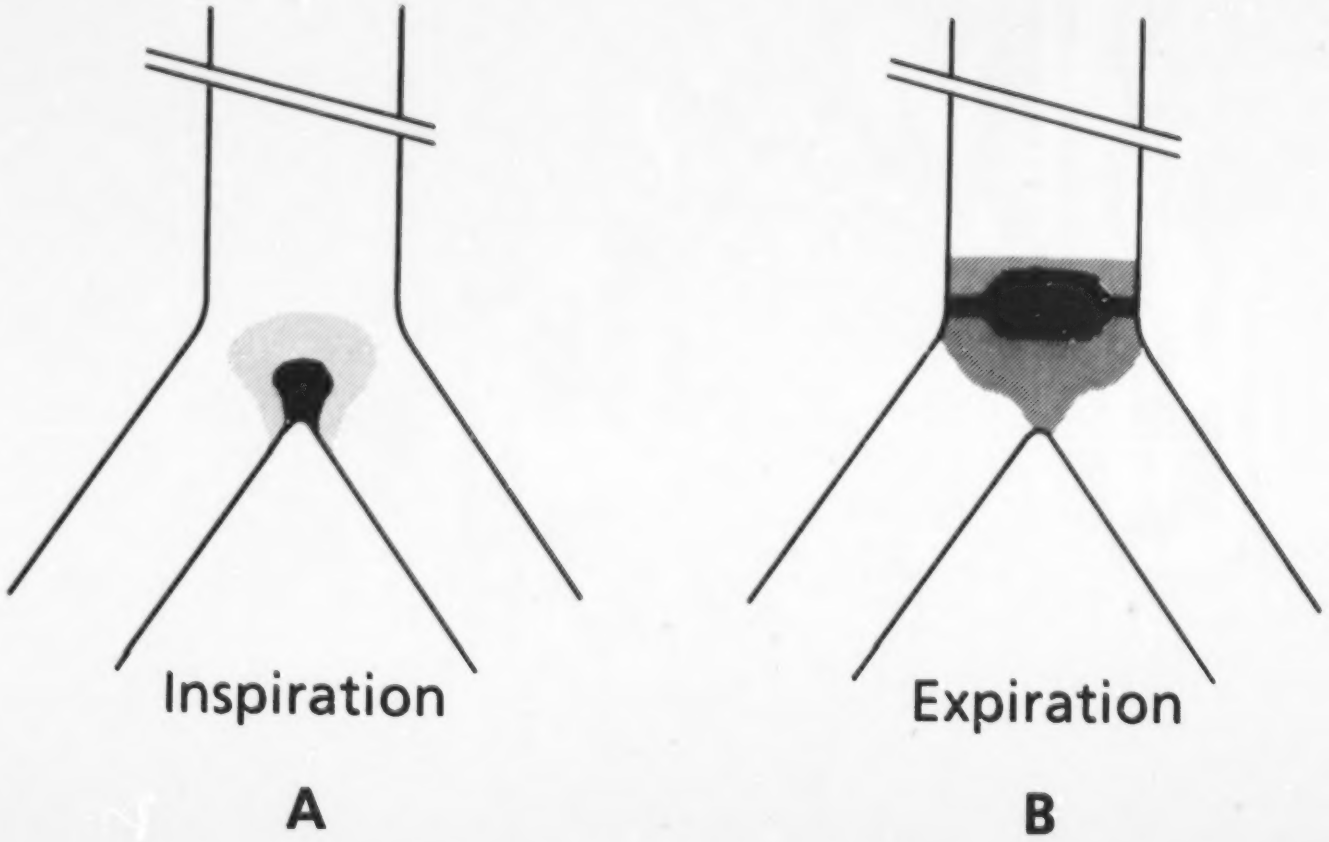

Figure 12. Graphic artist's representation of the deposition pattern of 7 μm (MMAD) monodisperse aerosols at a trachea-main bronchi juncture: (A) inspiration, (B) expiration.

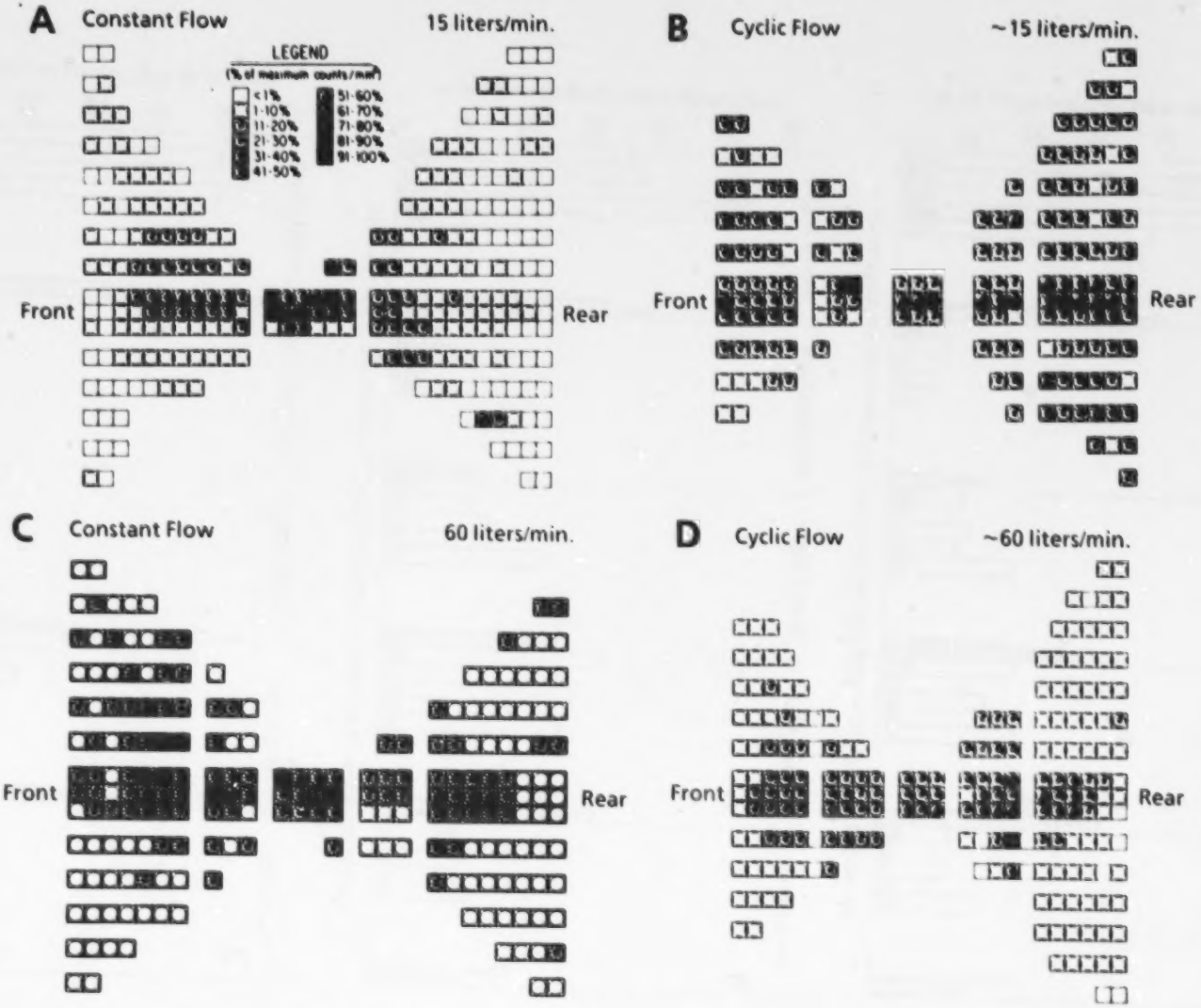

Figure 13. Mapping of the distribution of 8 um (MMAD) monodisperse aerosols within a bifurcation dissected from a replica tracheobronchial cast (from Schlesinger et al. (4). (A) constant flow, 15 $Lmin^{-1}$. (B) cyclic flow, 14 $Lmin^{-1}$ (mean). (C) constant flow, 60 $Lmin^{-1}$. (D) cyclic flow, 65 $Lmin^{-1}$ (mean).

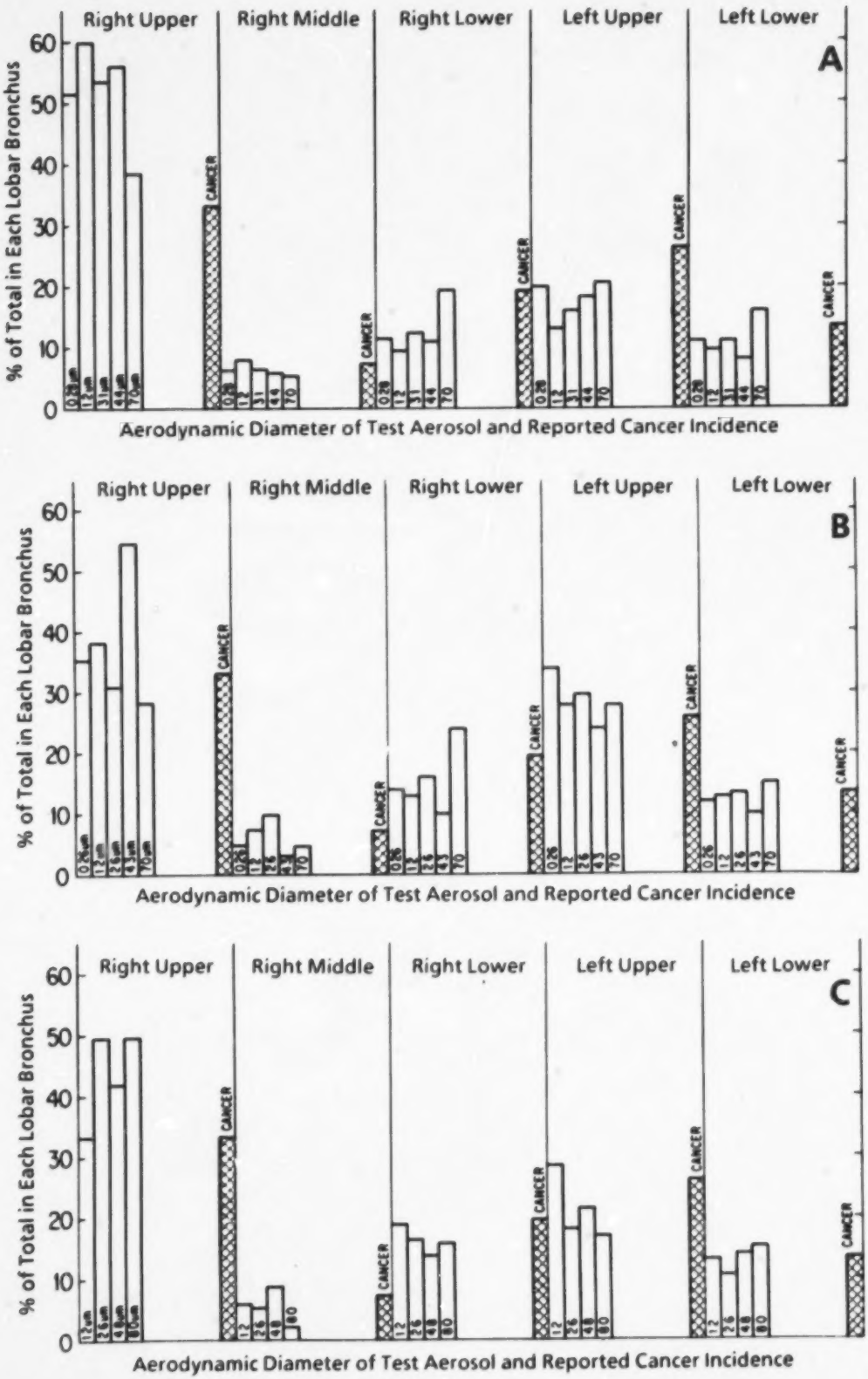

Figure 14. Distributions of total lobar-deposited aerosol activities among the five lobar bronchi of the human lung and the clinically observed incidences of total lobar carcinomas occurring at each bronchus (from Schlesinger and Lippmann (31)). Panels A, B, and C. refer to constant inspiratory flow rates of 15, 30 and 60 $Lmin^{-1}$, respectively.